

MSc. thesis:

Characterizing the ice-ocean interaction  
at the Upernavik Glacier  
using in-situ and satellite observations

by Dóra Kovács

*Supervisors:*



**Andreas P. Ahlstrøm**

Geological Survey of Denmark and Greenland



**GEUS**

Department of Glaciology and Climate



**Aslak Grinsted**

University of Copenhagen



Centre for Ice and Climate

University of Copenhagen, 04.09.2018.

# Acknowledgement

---

First and foremost, I would like to thank my two supervisors, Andreas P. Ahlstrøm and Aslak Grinsted their guidance and flexibility. I would especially like to thank Andreas for taking me as a student when I approached him out of the blue, for his help with finding a project for me and for introducing Aslak to me. I also greatly appreciate the encouragement I have gotten regarding my poster presentation at the IASC Network on Arctic Glaciology Annual meeting in Austria, it was a memorable experience. I thank Aslak for sharing some of his brilliant computer and coding skills and for being patient with me and my less-so-brilliant coding skills.

I would like to thank the Centre for Ice and Climate at the Niels Bohr Institute and the whole department of Glaciology and Climate at GEUS. A special thank you goes to Signe Bech Andersen for accepting me as a student, for Signe Hillerup Larsen, Nanna B. Karlsson and Karina Hansen for helping me getting started and for answering my many, technical questions. I would also like to thank Jason E. Box, William Colgan, Kristian Kjellerup Kjeldsen and Anne M. Solgaard for helping me out with very random questions.

A huge thank you goes to my family and my friends who supported me along the writing process. I would especially like to thank my mom, my brother and Andras for encouraging and supporting me, Santosh for never being tired of my MATLAB questions regardless the time of day and Jurriaan for his very deep and complex scientific thoughts that inspired me along the way.

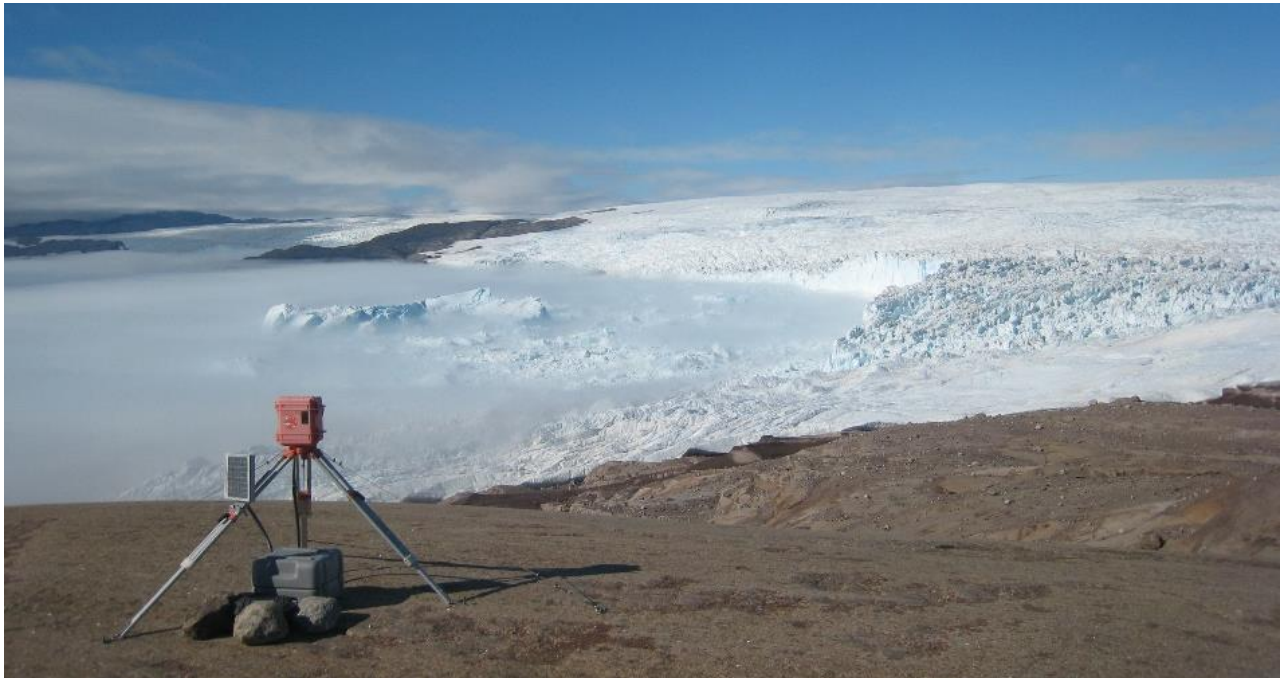
# Abstract

---

Former observations of tide-water glaciers showed extensive glacier flow velocity accelerations in the past decades and the high flow speed is expected to characterize the upcoming years as well (Rignot, Velicogna, Van Den Broeke, Monaghan, & Lenaerts, 2011). Combining data from satellites and time-lapse imagery, near terminus flow velocity fluctuations were analyzed at the northernmost branch of the Upernavik ice stream in north-west Greenland over August 2014. Measurements of atmospheric parameters recorded by in-situ automated weather stations were related to the observed flow speed variations and to calving events in order to learn more about their interactions and to find possible links between them. The data revealed a strong positive correlation between ablation change and velocity change that is in alignment with earlier reports (Van De Wal et al., 2008). The near terminus surface area grew by 0.0854 km<sup>2</sup> between 30.07-31.08.2014. In the same time-period, calving was captured by the camera on eleven days. Days when the glacier calved were most of the time (8 days out of 11) either preceded by or occurred on the same days as faster than average flow. This agrees with previous expectations, as calving events and increased flow are often in tune (e.g. Khan et al. 2013). Although, it had been concluded by others that ice front retreat and seasonal flow acceleration does not coincide (Lemos et al., 2018). Several other authors warned against oversimplification when examining the complex relationships in the context of glacier flow, warm induced surface

melting, calving and their feedbacks. The driving mechanisms behind these processes are yet to be confirmed.

**Keywords:** glacier-ocean interaction, calving, satellite and time-lapse imagery



Extreme Ice Survey camera facing the terminus of the northernmost branch of the Upernavik glacier.

# Table of contents

---

- Introduction..... - 4 -
  - Aim of study..... - 4 -
  - Relevance ..... - 4 -
  - Importance ..... - 5 -
  - Structure of the thesis..... - 9 -
- Theory and background ..... - 10 -
  - Glen’s Flow Law:..... - 11 -
  - Factors controlling movement and flow velocity:..... - 14 -
  - Flow velocity:..... - 15 -
  - Surface mass balance and response time: ..... - 16 -
  - Glaciers’ role in the hydrological cycle:..... - 20 -
  - Calving and ice margin stability:..... - 20 -
  - Effects on sea level and climate: ..... - 22 -
- Study area..... - 23 -
  - Climate:..... - 25 -
  - Glacier terminus position variation in the past:..... - 26 -

Ice flow velocity:.....	- 28 -
Methods .....	- 28 -
Surface area change .....	- 28 -
Weather parameters .....	- 29 -
Glacier velocity .....	- 30 -
Results .....	- 35 -
Surface area change .....	- 35 -
Weather parameters .....	- 37 -
Air temperature:.....	- 37 -
Cloud cover:.....	- 38 -
Air pressure: .....	- 39 -
Wind speed:.....	- 40 -
Other factors: .....	- 41 -
Calving events.....	- 42 -
Glacier velocity .....	- 45 -
Relationship between weather parameters and glacier velocity .....	- 50 -
Discussion .....	- 53 -
Surface area change .....	- 54 -

Weather parameters .....	- 54 -
Glacier velocity .....	- 57 -
Ablation and glacier velocity .....	- 60 -
Role of sea .....	- 63 -
Conclusion and future work .....	- 65 -
References .....	- 69 -
Appendix.....	- 76 -
Camera data .....	- 76 -
MATLAB codes.....	- 76 -
Camera fitting:.....	- 76 -
Tracking pixel displacement.....	- 78 -
Looping the images one after the other .....	- 79 -
Pairing velocities between two consecutive days:.....	- 79 -
Calendar plot: .....	- 80 -
Comparison to Terra SAR-X:.....	- 81 -
Correlating parameters (substitute for the desired parameter): .....	- 82 -
Weather station data .....	- 83 -

# Introduction

---

## Abbreviations

- UI = Upernavik ice stream
- UPE1 = northernmost branch of UI
- GrIS = Greenland Ice Sheet
- NAW = North Atlantic Waters
- DEM = Digital Elevation Model
- EIS = Extreme Ice Project (time-lapse images)
- SMB = Surface Mass Balance
- ELA = Equilibrium Line Altitude

## Aim of study

Climate change is a hot debate topic of our days, Greenland and its elevated rates of ice loss is increasingly more in the spotlight. This study aims to investigate how glacier velocity changed within a month-long late summer period over August 2014, and to explore possible relations between glacier flow speed fluctuations and climatic factors in the northernmost glacier feeding the Upernavik isstrøm/Upernavik ice stream in north-west Greenland. Air temperature, air pressure, wind speed, cloud cover and ablation rate were investigated and related to the observed flow velocities looking for connections.

## Relevance

Upernavik ice stream is a major outlet glacier of the Greenland ice sheet (Larsen et al., 2016), a highly responsive region of the Earth to the climatic changes we are experiencing (Rignot, Velicogna, Van Den

Broeke, Monaghan, & Lenaerts, 2011). The behavior of tidewater glaciers (such as UI) has a great impact on global environmental systems including ocean temperature and thereby the ocean circulation patterns, which in turn influence air temperatures and wind patterns around the world (Knight, 1999), further enhancing the feedback mechanisms between climate and the ice sheet. Apart from the geophysical aspect, glaciers affect local ecosystems and communities that rely on the fresh water stored in glaciers and its periodic release (Moon., 2017).

This study is investigating the complex interactions between ice and its environment. UI was chosen as focus area, as this glacier system had been thoroughly studied before (e.g. Ahlstrøm et al., 2013; Andresen et al., 2014; Haubner et al., 2018; Khan et al., 2013; Larsen et al., 2016), resulting in a relatively high amount of data that was already available without the necessity of further field work.

The outlined scientific problem was explored with a short period, high-detail, high-sample-frequency approach, using a fairly new method for analyzing near-terminus glacier movements that may reveal characteristics that would not be obvious from more traditional analyses.

## Importance

Between 1993 and 2011 the greatest acceleration of ice sheet loss was observed in Greenland ( $21.9 \pm 1 \text{ Gt/yr}^2$ ), greater than in Antarctica and almost twice as much as in mountain glaciers and ice caps combined (Rignot et al., 2011). As a result, ice loss from the GrIS contributed most to sea level rise globally in the past two decades and can be the dominant source for further sea level rise in this century. Sampling more than 200 major Greenlandic outlet glaciers over a decade, *Moon et al., 2012*

suggest a sea level rise contribution of 9.3 cm by 2100. Ice mass loss originating from the GrIS can potentially alter the Atlantic Meridional Overturning Circulation, the regional circulation as well as sea-ice formation and ocean-air interaction (Straneo, 2017).

While in the period from 2000 to 2008 GrIS mass loss added 0.46 mm/yr to the global sea level (van den Broeke et al., 2009), in 2011-2014 this contribution rose to  $0.74 \pm 0.14$  mm/yr (McMillan et al., 2016). Locally at UI, based on recent simulations, thinning and acceleration were responsible for 70 % of the total mass loss between 1849 and 2012 (Haubner et al., 2018) and this accelerated shrinking is typical for the whole GrIS (Moon 2017; Moon et al. 2012). In north-west Greenland, where UI is located, between 2000 and 2010 a relatively steady acceleration of 28% was observed (T. Moon et al., 2012). According to *Howat & Eddy, 2011*, out of 210 marine-terminating glaciers in Greenland, 90% of them retreated between 2000 and 2010, this ratio approaching 100% in the north-western part of the ice sheet margin.

At Upernavik this meant a loss of 7.9 square kilometers of ice per year from the combined termini of all four branches of the ice stream (Box & Decker, 2011). Tidewater glaciers, valley glaciers that terminate in the sea (Knight, 1999), played a major part in this recent mass loss, as they respond readily to ocean water and air temperature fluctuations (Andresen et al., 2014; Bevan et al., 2012). It is disputed whether climatic and ice sheet-ocean interactions are the primary controls of mass loss over whole regions (Murray et al., 2010), or if local factors may be prevalent. The latter could explain asynchronous behaviors between adjacent glaciers, as observed between the four branches of UI (Larsen et al., 2016; Moon et al., 2012; Nick et al., 2012). It had previously been suggested that bed-,

glacier- and fjord geometry (Howat et al., 2007), ocean water flow (Scambos et al., 2017; Shepherd et al., 2004), local climate and sea ice conditions at the terminus are all influencing glacier behavior (Moon et al., 2012). According to *van den Broeke et al., 2009* surface processes and ice discharge are equally responsible for mass loss in northwest Greenland, while a very recent simulation study by *Haubner et al., 2018* suggests that the dynamic response to terminus position change at UI was the dominant factor for 70% of the total simulated mass change in the past 150+ years. Khan et al., 2013 estimated that ice dynamics were accountable for 79% of the total ice-mass loss at UI between 2003-2009. This indicates that a moving terminus position is a key component in the acceleration and thinning of UI (Moon & Joughin, 2008).

In the same region, warm North Atlantic waters ( $> 2.5$  °C) play an important role in ice discharge (Morlighem, 2017; Morlighem et al., 2014; Schaffer et al., 2016) by interacting with the glacier front, increasing submarine melting and undercutting, which can result in calving and an acceleration of ice flow (Pimentel et al., 2017). These processes are highly important, as submarine melt and calving are responsible for ca. 50% of the mean annual freshwater discharge from the GrIS (Mankoff et al., 2016). However, subglacial discharge plumes at the submerged base of marine-terminating glaciers can have a counter-effect during their rise towards the surface by impacting submarine melting and thereby iceberg calving and the fjord circulation (Mankoff et al., 2016).

Whether the warm NAW reach glacier fronts or not depends on complex geographic, atmospheric and ocean circulation patterns (Moon et al., 2012). Fjord bathymetry regulates the intrusion of warm ocean waters; the deeper the fjord, the further warm waters penetrate (Morlighem 2017). Unfortunately,

fjord bathymetry measurements are difficult to carry out due to the presence of icebergs. As a result of the deficient bathymetry data close to the calving front, existing numerical ice sheet models are often unprecise, representing the inner fjords as too shallow, and thus ignoring the importance of ice-ocean interaction (Rignot et al., 2016). Warm NAW are generally to be found deeper than 200-300 m below sea level (Morlighem, 2017; Rignot et al., 2016). Therefore, the presence of sills in fjords can prevent warm water to further penetrate and interact with glacier fronts. Although, that is not the case at UPE1, where the presence of a sill is unlikely, and water temperatures in the fjord were found to be more than 2°C between 300 and 700 m below the water surface (Andresen et al., 2014).

Some glaciers are simply grounded above the NAW zone (which may be the case more and more often if the retreating trend of glaciers continue and would do so at a higher pace than the accompanying sea level rise), or the fjords are not deep enough to host these waters (Morlighem et al., 2017). *Morlighem et al., 2017* suggest that there are 30-100% more glaciers that are potentially in contact with NAW, than previously thought. Given the NAW reach the glacier, the melting rate due to this contact will depend on the temperature of the ocean water, the slope and width of the interface, the distribution of plumes and the run-off volume (Larsen et al., 2016, Slater et al., 2015).

*Rignot, 2017* claims that the intrusion of this warm, salty, subsurface waters towards the coast, where they do come in contact with the ice sheet, melt the ice from below at rates orders of magnitude greater than at the surface. This is in agreement with what *Joughin et al., 2008* proposed, that instead of increased surface meltwater lubrication, recent outlet-glacier speedups were mainly related to

internal dynamics, processes that caused reduced back-stress and ice-front retreat, and the ratio of melt-induced speedup is only 10-15%.

Characteristics of bed rheology are also important for glacier velocity regulation, especially near the grounding zone, as a more plastic bed resists retreat for a longer time than a linear viscous bed<sup>1</sup>, but once started, the glacier will retreat more rapidly (Scambos et al., 2017). In the region around UI, the predominant bedrock is composed of a resistant, hard rock-type, granite (Dam et al., 2009).

## Structure of the thesis

In the beginning of this study relevant parts of the theory behind glacier flow will be covered, followed by a short introduction to the study area around the Upernavik glacier in terms of its location, climate and past terminus position changes.

Thereafter the results of this study's data analysis will be introduced with respect to surface area change, variations in different atmospheric parameters (these include air temperature and pressure, wind speed, cloud cover and ablation) and in glacier flow speed. This is followed by showing the results of correlating the weather parameter changes to glacier velocity fluctuation.

Next, the results will be discussed in the view of previously conducted studies, where agreements and disagreements are presented.

---

<sup>1</sup> <https://www.see.leeds.ac.uk/structure/rheology/viscous.htm>

In the last section the conclusions of this thesis are summed up with recommendations regarding improving the data quality and concerning potential future work.

## Theory and background

---

*„A glacier is a body of ice originating on land by the recrystallization of snow or other forms of solid precipitation and showing evidence of past and present flow” – Meier, 1964*

The vast area of land covered with a thick ice layer makes the ice-covered part of Greenland the Greenland ice sheet (GrIS), that is by definition *A layer of ice covering an extensive tract of land for a long period of time<sup>2</sup>, often larger than 50.000 km<sup>2</sup> (Knight, 1999).*

The role of glaciers in past and future changes in the Earth system is vital. Their interaction with climate, the hydrological cycle and the ocean-atmosphere circulation changes our environment on a global scale. Therefore, regarding our future prospects in the heavily debated topic of climate change and sea level rise it is fundamental to have a deeper understanding of how glacier systems work.

Firstly, it is vital to understand glacier movement. Glacier movement have three components, plastic deformation of ice (regarding ice as a perfectly plastic material), sliding of ice over the glacier bed and the deformation of the glacier bed. The latter two combined are often defined as basal motion. Sliding occurs only when the basal ice is at its melting point, whereas bed deformation is only significant if it

---

<sup>2</sup> [https://en.oxforddictionaries.com/definition/ice\\_sheet](https://en.oxforddictionaries.com/definition/ice_sheet)

consists of sediments with water at a pressure similar to that exerted by the ice lying on top (Paterson, 2002).

As per the definition of Knight, 1999 the deformation of ice *refers to changes in the shape of a region of glacier ice in response to stress and can consist of creep (a deformation that results from movement within or between individual ice crystals) or fracture (brittle failure that occurs when ice cannot creep fast enough to allow a glacier to adjust its shape under stress often resulting in crevasse formation).*

Unlike in rocks, deformation in glaciers has only one driving force, gravity (Paterson, 2002).

Glen has found that ice deforms permanently when constant stress is applied on it. The rate of deformation is however time dependent, after a few hours, the rate of deformation slows down to a steady value. It was also found that the rate of strain is small when shear stresses are low, and it grows rapidly when increased shear stresses are applied. Therefore, a small increase of stress will result in a large increase in strain rate (Nye, 1952).

Glacier flow itself is defined by Glen's Flow Law as the following (from Knight, 1999):

Glen's Flow Law:

$$\varepsilon = A * \pi^n$$

$\varepsilon$  = strain rate (amount of deformation)

A= ice hardness parameter, depends largely on temperature

$\pi$ = stress deviator (driving force)

n= power law constant, often given as n=3

The Flow Law describes the relation between the applied force, stress and the deforming response, strain. This relationship is essential for glaciology, as it defines how ice is deformed under stress. Every single ice crystal starts to deform elastically to a certain extent when stress is applied to them. As the stress ceases, the ice recovers unless the elastic limit or yield strength is reached. In that case permanent plastic deformation or creep begins and lasts until the stress is removed, generally by slipping on the crystal's basal plane. With respect to greater, polycrystalline ice masses, deformation of these aggregates involves other processes as well, such as intergranular adjustment that is the movement of single crystals relative to one other and recrystallization. As a result, crystals often become reoriented, the basal planes of individual crystals being parallelly aligned with the direction of the driving stress (Knight, 1999).

The driving stress  $\tau_b$  is a function of the weight of the ice and the gradient of the surface driving the ice movement. The driving stress can be described as (from Cuffey and Paterson, 2010):

$$\tau_b = \rho * g * h * \sin\alpha$$

where  $\rho$  = ice density;  $g$  = acceleration due to gravity;  $h$  = ice thickness;  $\alpha$  = gradient.

As per *Knight, 1999*, for strain is proportional to the cube of stress ( $\pi^3$ ) and stress is proportional to depth, most of the strain is present in the lower section of the ice profile. This deformability of ice in the lower sections is enhanced by the effect of temperature in the Flow Law ( $A = A_0 \exp[-\frac{Q}{kT}]$ ) since ice hardness is temperature dependent and the temperature commonly increases towards the glacier

bed. Motion in the lower parts of the glacier pushes ice towards the surface and thereby the velocity at depth is transmitted upwards. At the surface, ice motion is a cumulative function of the total strain through the depth of the ice column, causing the velocity to be greatest at the surface. Glacier surface velocity is defined as: *a measured rate at which a glacier is moving downhill under the influence of gravity, through the processes of sliding on its bed and internal deformation of the ice.* (Singh, Singh, 2001).

According to *Paterson, 2002*, depth-averaged flow velocity is generally between 80-90 % of the surface velocity.

As described by *Knight, 1999*, in ice sheets, summits act as ice-divides and ice flows outwards from these areas as a response to a stress gradient that is largely ascribed to the topography profile. They define how large of an area can be potentially drained through a particular glacier. The locations of these ice divides are not constant and therefore, their migration can result in a lack of mass balance by increasing/decreasing the accumulation area of glaciers, driving fluctuations in glacier front positions. In case of Greenland, the main ice divide extends in an almost north-south direction<sup>3</sup>, all across the island.

---

<sup>3</sup> [http://www.iceandclimate.nbi.ku.dk/research/flowofice/modelling\\_ice\\_flow/](http://www.iceandclimate.nbi.ku.dk/research/flowofice/modelling_ice_flow/)

## Factors controlling movement and flow velocity:

The main controls on flow velocity are: topography, thermal regime, presence of water and its pressure, bed rheology and its rigidity and ice crystal size and their orientation (Knight, 1999).

### Subglacial topography:

In areas where the ice is thin such as near the margin, subglacial topography is the key factor influencing glacial movement. *Knight, 1992* found that at the margin of the GrIS, ice deformation and movement was closely dependent on ice flexure over subglacial obstacles.

### Presence of water:

Water acts as a lubricant, promoting the sliding of glaciers. In terms of short term glacier velocity fluctuations, the role of water, namely the distribution and pressure of water at the bed is crucial. During periods of greater motion, the basal water pressure is generally higher (Willis, 1995). Water can submerge minor (mm scale) obstacles making the bed smoother and thus promote sliding. At a larger scale, pressurized water in cavities can also reduce bed roughness.

### Ice temperature:

*Knight, 1999* discussed that the temperature within glaciers is not uniform but vary in space and time. The melting point of ice is decreasing as the mass lying upon it is increasing, at a rate of  $0.072^{\circ}\text{C}$  per million Pascals. Consequently, the melting point of ice is referred to as the pressure melting point. This temperature is important as glaciers only move if the ice is at or close to the melting point. The factors controlling ice temperature and its distribution are the following: surface temperature that is related

to climate; geothermal heat, friction, and the refreezing of meltwater warming the interior. Heat within the ice is transferred by ice movement, conduction and water flow (Paterson, 2002).

### Flow velocity:

The flow velocity of glaciers is rarely constant for long periods of time, preventing a stable, steady-state flow. The glacier front's position is stable if the amount of ice supplied to the front from up-glacier equals the amount that is lost at the front. If this balance becomes unstable, the glacier either advances at the event of increased supply or retreats when ice loss exceeds the supply. The reason for the ice margin position change is to maintain mass equilibrium at the margin, where ice loss would balance out the accumulation. Mass imbalance at the terminus can be linked to changes in ice dynamic conditions or to fluctuations in climate-related mass balance (e.g. Stocker-waldhuber et al., 2018, Straneo, 2017, Knight, 1999). Glacier response to these changes is however not instantaneous and different glaciers have different reaction times (Willis, 1995). Therefore, if the factors causing the imbalance are frequently changing, the 'normal' or regular state of the glacier might be the disequilibrium. As argued by *Knight, 1999*, variations in glacier size can occur in a wide range of time scales from days to millions of years. Long term margin position fluctuations are generally related to mass balance changes. Short term variations on the other hand can be explained by local variations of sliding dynamics, by surges or by the life cycle of ice streams. Terminus advance and retreat can be observed on a seasonal time scale that is associated with seasonal changes in local ice loss caused by for example meltwater availability or subglacial environment changes (Moon et al., 2014). Seasonal

velocity fluctuations however seem to be of minor importance regarding the mass balance of entire ice sheets (van den Broeke et al., 2009).

Velocity is generally highest during summer when the ice is warmer and there is a greater amount of basal meltwater present, however that is not always the case (Willis,1995). When air temperatures are higher, the ice temperature also increases which in turn reduces basal friction and thus accelerate glacier motion. Flow rates are also elevated if precipitation increases, thickening the ice mass (Knight, 1999).

Regarding velocity fluctuation in the summer period which this study is focusing on, *Müller and Iken, 1963* highlighted the importance of water present in the glacier. They found that glaciers with low discharge capacity can experience a substantial velocity increase when run-off fluctuations are large and frequent even if the melt is relatively low, as the ground-water level in the glacier rises fast, but the decrease is slow. Gradual increases in water supply has therefore less effect on glacier velocity, than sudden ones. In agreement with the above, *Moon et al., 2015* concluded that the subglacial hydrology of marine-terminating glaciers may be of great significance in terms of seasonal velocity changes.

### Surface mass balance and response time:

Climatic variations – mainly temperature and precipitation changes- affect the length and thickness of glaciers. The mass balance of a glacier is the difference between the input and output, in other words

the snow that has fallen in the winter (accumulation) and the snow and ice that was lost in the summer (ablation)<sup>4</sup>. So that we can write:

$$b = c + a = \int_{t_1}^t (c + a) * dt$$

where  $b$  is the cumulative mass balance,  $c$  is the sum accumulation  $a$  is ablation- defined here as negative.<sup>5</sup>

*Accumulation: all processes by which snow or ice are added to a glacier, this is typically the accumulation of snow, which is slowly transformed into ice; other accumulation processes can include avalanches, wind-deposited snow, and the freezing of rain within the snow pack.*<sup>6</sup>

*Ablation: Output or ablation includes all the ways in which mass is lost from a glacier: melting, evaporation, wind deflation and iceberg calving being the most important (Souchez and Lorrain, 1991).*

---

<sup>4</sup> [https://www2.usgs.gov/climate\\_landuse/clu\\_rd/glacierstudies/massBalance.asp](https://www2.usgs.gov/climate_landuse/clu_rd/glacierstudies/massBalance.asp)

<sup>5</sup> [https://glaciers.gi.alaska.edu/sites/default/files/mccarthy/Notes\\_massbal\\_Hock.pdf](https://glaciers.gi.alaska.edu/sites/default/files/mccarthy/Notes_massbal_Hock.pdf)

<sup>6</sup> <https://nsidc.org/cryosphere/glossary>

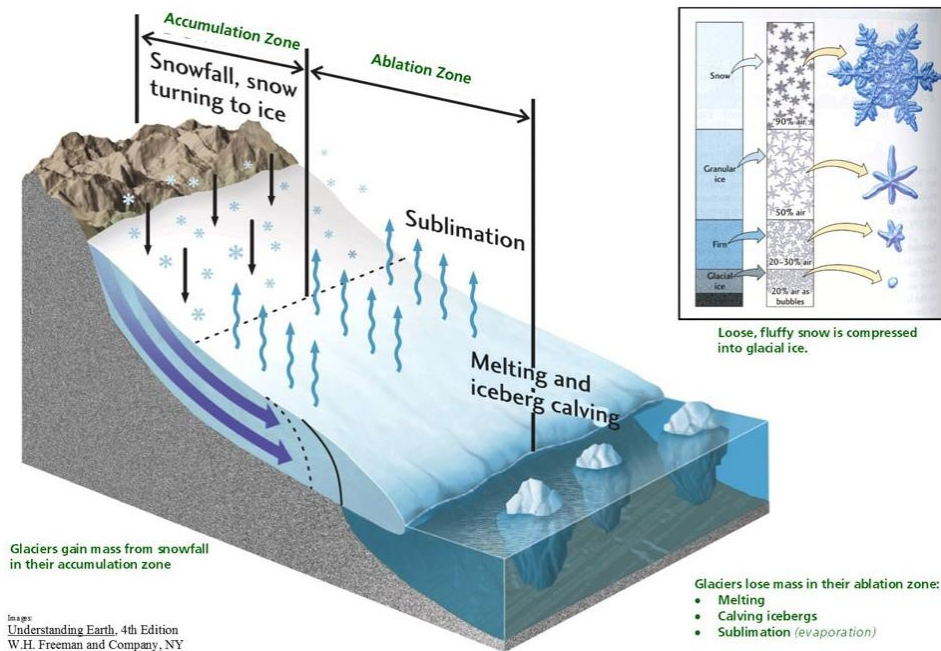


Figure 1.: Accumulation and ablation zone of a glacier. Dotted line represent the equilibrium line. Image from: <https://www.nps.gov/glba/learn/nature/anatomy-of-a-glacier.htm>

The annual mass balance is positive, if more snow or ice accumulated in the cold winter months, than the amount that was lost in the summer. SMB is not only temperature and hence time dependent, but also space dependent, as accumulation is typically greater at higher altitudes than in the lower, warmer areas of the glacier.

The boundary, where accumulation equals ablation is called the equilibrium line. Here, the SMB is zero<sup>7</sup>.

<sup>7</sup> <https://nsidc.org/cryosphere/glossary/E>

Understanding the SMB systems of glaciers is important, it can help us identifying connections between climate change and glacier behavior.

Thus, information on accumulation and ablation rate are crucial. Unfortunately, there are no stations installed measuring precipitation locally, in the vicinity of UPE1, therefore accumulation is not discussed further in this report.

Ablation rate is important for establishing the SMB of a glacier, which in return can yield valuable information on the responses the glacier has to changes in the weather and climate, which might be indicative of possible responses to long-term climatic changes over longer periods.

The time elapsed for a glacier to react to a change in its mass balance is called the response time. It is determined by the glacier volume  $V$ , the area  $S$ , and the mass balance,  $b$  and can be calculated as (from *Paterson, 2002*):

$$t = V_1 / (\bar{b}_1 * S_0)$$

where the 0 suffix denotes the original state and the 1 suffix refers to the perturbation.

*Müller and Iken. 1963* found that in the beginning of the summer, the time lag between ablation and velocity change was between 2-5 days, whereas from July on, the lag was no more than a few hours.

In this thesis, the connection between temperature change and ablation, as well as the relationship between ablation and glacier velocity has been investigated. It is however important to emphasize that the focus period of this study is very short with respect to time scales of overall changes in a

glacier system for reacting to changes in the climate and any extrapolation should be treated with caution.

### Glaciers' role in the hydrological cycle:

As per *Knight, 1999*, fresh water is contained in glaciers with an average residence time of 10,000 years. After being released from the glacier, water is transferred back to the hydrological cycle via ablation. This transfer can happen in several forms: the ice can melt and flow in surface streams terminating directly in the ocean, it can flow underground, alternatively it can also evaporate or sublimate to the atmosphere. A large amount of ice is being lost through calving at the glacier front, that will eventually melt, and increase the amount of water in the ocean basins that can result in sea level rise. This is a straight forward relation, however reality is more complex than this.

### Calving and ice margin stability:

In Greenland, ca. 30% of the total ice mass was lost by calving between 2011-2014<sup>8</sup>. Calving is *the production of icebergs by detachment of ice from a parent glacier terminating in water. The calving zone of a tidewater glacier margin coincides with the grounding line* (Benn and Evans, 2006).

Penetration of meltwater into crevasses from the surfaces of tidewater glaciers during summer can create or widen areas of weakness in favor of calving (Paterson, 2002). Calving occurs when the tensile stresses pulling a piece of ice away from the glacier margin become greater than the strength of ice.

---

<sup>8</sup> <https://www.sciencemag.org/news/2017/02/great-greenland-meltdown>

This process is typical for the summer period in Greenland and is responsible for a large part of ablation, when a glacier is in contact with deep water (Benn and Evans, 2006). When the calving front is in deep water, waves and currents may remove ice from the front by undercutting, promoting rapid calving and hence, glaciers can become unstable resulting in fast retreat (Paterson, 2002). Thus, as topography has a great influence on ice margin stability, glacier response to climatic changes are often non-linear. The behavior of a particular calving glacier is primarily determined by the terminus position within the local topography (slope of the bed and whether the ice is in contact with ocean water) and will only to a lesser extent depend on the magnitude of the given climatic signal (Benn and Evans, 2006). At glaciers where the bed slopes away from the glacier terminus and the glacier becomes thicker due to for instance increased precipitation, the grounding line will move to a more advanced position into deeper waters, that may result in higher calving rates.

Nevertheless, glacier development is strongly dependent on both the local topographic and the climatic environment as these conditions determine whether snow and ice would survive from one year to the next. After analyzing ice front changes of 203 glaciers, *Moon & Joughin, 2008* concluded that tidewater retreat is strongly linked to climatic changes through elevated retreat rates during warmer periods. With respect to climate, the key component is the energy available to melt ice, that is often related to air temperature (Benn and Evans, 2006). Although mean annual temperatures do not reflect the degree of glacierization, the number of positive degree-days - days when temperatures are greater than 0°C- is closely linked to the amount of ablation (Cuffey and Paterson, 2010). Less ice will survive in a year with a higher number of positive degree-days compared to colder years.

## Effects on sea level and climate:

The total sea level rise potential of the GrIS is  $7.42 \pm 0.05$  m (Morlighem et al., 2017). It is also known that the globally averaged land and ocean surface temperature rose by  $0.85$  °C from 1880 to 2012 (IPCC, 2013), while the Arctic, north of  $60^\circ$  N, warmed more, by ca.  $3.5$  °C (Overland et al., 2016).

In terms of sea level change, we can distinguish between isostatic (local) and eustatic (global) sea levels. The amount of water in the ocean basins alone is not the sole control on sea level. The shape of the geoid, the gravitational force exerted by large masses - such as the ice sheet of Greenland - and isostatic conditions, hence the variation in the rheology of the Earth's crust and its non-uniform response to regional loading also regulate water levels at the coastal parts of the planet. This vertical crustal movement is however mostly relevant on a larger time scale than what is discussed in this study (*Brink, 1974* reports a rebound rate of  $60\text{-}105$  m / 1000 years in west Greenland).

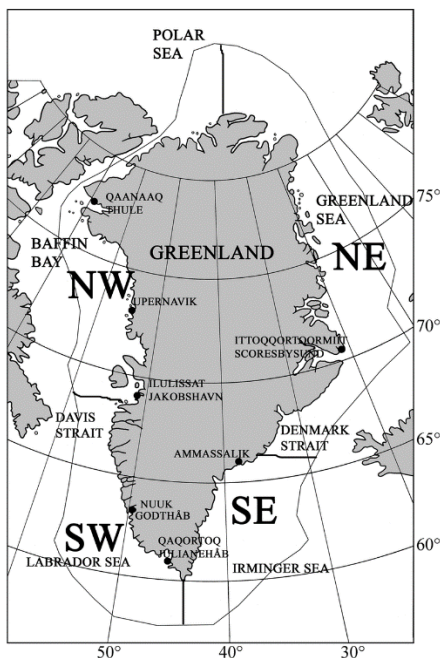
Ice loss in Greenland has been accelerating rapidly in the past years without any prospect of this trend to change. Between 2003 and 2013, the GrIS ice loss acceleration was ca.  $25 \pm 1.2$  Gt/year (Velicogna et al., 2014), with an ice loss of ca. 360 Gt/year between 2003 and 2009, that translates to a sea level contribution of  $0.8 \pm 0.2$  mm/year (Moon et al., 2018).

The effect of glaciers on sea level is not unidirectional. Sea level, ocean temperature and circulation patterns also influence the stability of tidewater glaciers, just as glaciers have an impact on all these factors in return by changing the volume, composition, temperature and circulation of ocean waters (Allison et al., 2009).

Glacier response to changes in the climate is very complex and therefore difficult to predict. Elevated air temperatures can facilitate increased ablation at ice sheet margins. Interestingly, however, central Greenland ice core data show that not only ablation can be greater with higher surrounding air temperatures, but also the accumulation due to increased precipitation on the ice sheet (Knight, 1999) that is typical for warmer periods. Thus, global warming could counterintuitively result in ice-sheet growth.

## Study area

Figure 2.: Map of Greenland (modified from Moeller et al. 2010).



Upernavik ice stream is a major outlet glacier of the Greenland ice sheet in the north-western part of Greenland (Figure 2.). Paterson, 2002 defines an ice stream as a region in a grounded ice sheet in which the ice flows much faster than in the regions on either side. The majority of the discharge in Greenland is transferred via ca. 20 large outlet glaciers, therefore the state of the ice sheet is largely controlled by these ice streams. In terms of velocity, usually it is increasing from up-glacier all the way down to the glacier terminus, having a maximum velocity there. It is important to note

however that the behavior and characteristics of individual ice streams can vary within a broad range (Cuffey and Paterson, 2010).

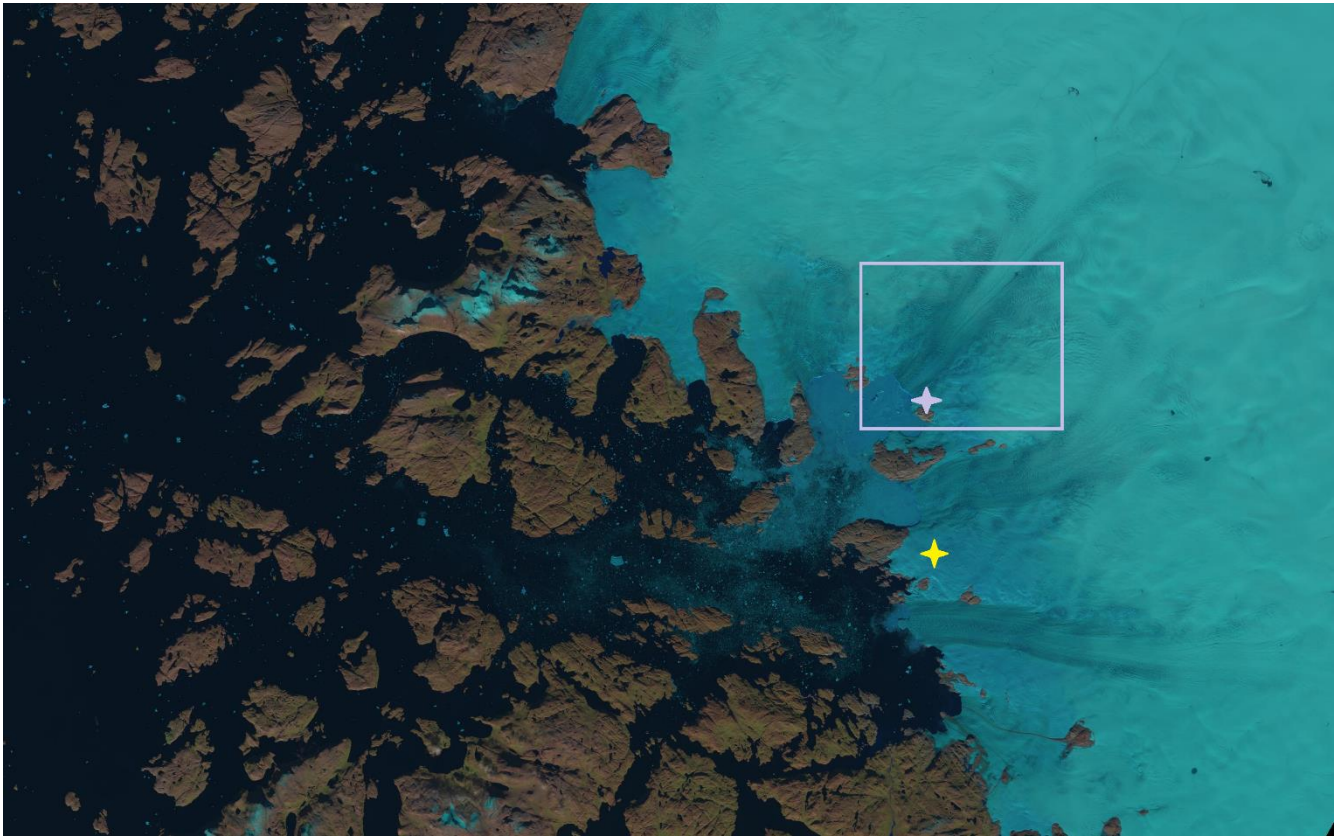


Figure 3.: Landsat 8 image over the Upernavik ice stream. The rectangular box marks the glacier front of UPE1, the purple star indicates the camera location, the yellow star marks the location of the automated weather station. (Landsat image from: <https://earthexplorer.usgs.gov>).

The Upernavik ice stream consists of four major fast flowing outlet glaciers (UPE1-4) terminating in the Upernavik Icefjord. Before 1980, the glaciers had a single terminus<sup>9</sup>. Most of the discharge - of the total discharge of  $53.5 \pm 12.8$  Gt between 2005–2010 (Khan et al., 2013)- is occurring through UPE1 and UPE2, the two northernmost glaciers of the four (Andresen et al., 2014). In the same time-period, a marked speed-up of the northernmost glacier was observed, along with thinning and retreat.

---

<sup>9</sup> <https://blogs.agu.org/fromaglaciersperspective/2017/05/30/upernavik/>

Therefore, UPE1 was chosen to be the focus of this project, marked in *Hiba! A hivatkozási forrás nem található.* The Upernavik icefjord is ca. 80 km long and most of it is more than 900 m deep, with approximately 400-600 m depths near the glaciers' front (Morlighem 2017). The terminus of UPE1 is ca. 3.5 km wide and up to approximately 100 m high above sea level<sup>10</sup> (from ArcticDEM data).

The temperature profile of the fjord itself is layered (Andresen et al., 2014): ca. 2°C in the top 50 m with low salinity values, 0.5–1.5°C between 50-150 m and below that the temperature gradually rises from 1 to 3 °C along with growing salinity, indicating the presence of the Atlantic water in the bottom of the fjord. With a 400-700 m deep grounding line of UPE1-3, it is suggested that the relatively warm Atlantic water is in contact with the glacier fronts, influencing retreat patterns.

UI is a type 2 glacier (Moon et al., 2014), that is characterized by relatively stable velocities from late summer to spring, a strong early summer speedup and a midsummer slowdown.

## Climate:

The area around the town Upernavik (72.7863° N, 56.1376° W) has a tundra climate. Winters are long and cold in the region with a relatively small amount of precipitation while summers are mild with July being the hottest month with an average temperature of 5.6 °C. The temperature is generally below 0°C for as long as 8 months per year. August is considered a warm month with an average temperature

---

<sup>10</sup> <https://www.pgc.umn.edu/data/arcticdem/>

of 5.5 °C, and a precipitation of ca. 27 mm, followed by the wettest month of the year (35 mm precipitation). The yearly average rainfall is 220 mm.<sup>11</sup>

### Glacier terminus position variation in the past:

The front position changes at Upernavik icefjord are illustrated in *Figure 4.* covering a period between 1849-2010.

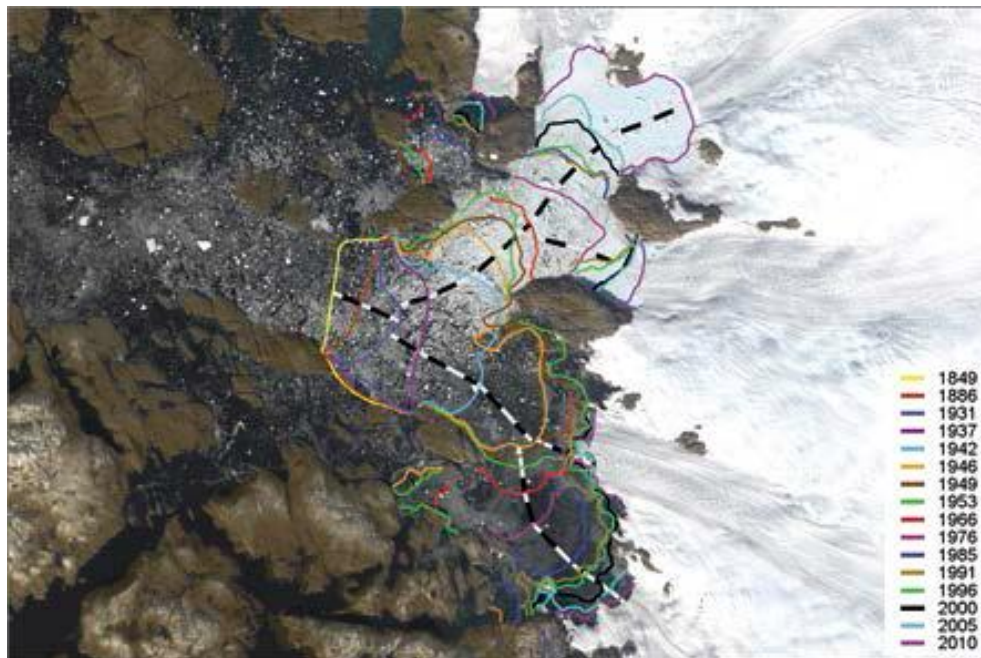


Figure 4.: Glacier terminus position changes between 1849-2010 (from Andresen et al., 2014)

---

<sup>11</sup> <https://en.climate-data.org/location/274141/>

From the Little Ice Age (ending in ca. 1850)<sup>12</sup> until about 1931, UPE1-4 was a single glacier with a low retreat rate. This retreat gained speed in 1931 and lasted until the mid '40-s, when retreat rates lowered again. UPE1 became a separate glacier in 1966 and experienced increased retreat between 1966-1985, in the late '90-s and between 2005-2009, where the retreat was outstandingly fast accompanied by a marked thinning. Interestingly, the other three glaciers showed a different behavior and their retreat rates remained slower in the period of 2005-2009 compared to UPE1 (Andresen et al., 2014). The above mentioned fast-retreat periods coincided with elevated air temperatures near Upernavik and entire Greenland (Chylek et al., 2006).

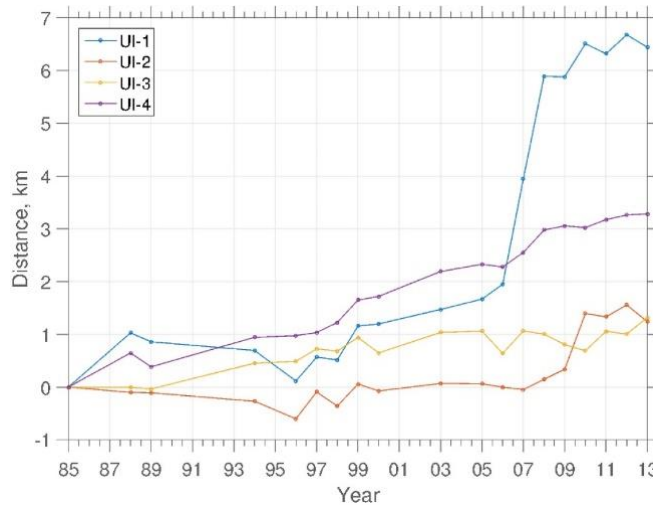


Figure 5.: The distance from the 1985 calving front position. UPE1 is denoted as UI1, marked with blue (from Larsen et al., 2016).

The rapid retreat of the glacier margin at UPE1 in the mid-late 2000s is depicted in *Figure 5*. It is clearly visible that the retreating pattern started in 1996 and continued with relatively minor fluctuations-

<sup>12</sup> <https://www.britannica.com/science/Little-Ice-Age>

however, at a notably lower rate- until 2013, the year before this report's focus period, resulting in a retreat of ca. 6,5 km relative to the glacier front position in 1996.

### Ice flow velocity:

According to *Larsen et al., 2016*, glacier velocities were stable between 1992-2005 at UPE1, flow acceleration and thinning started in 2006. This pattern continued until 2011, thereafter the acceleration stopped, and the flow speed stabilized until 2013. The authors also suggested that UPE1 had had a floating tongue between 1985-2007 that fragmented and broke off between 2007-2008 likely due to ocean-warming in the late 1990s, destabilizing the glacier, causing the rapid acceleration and thinning.

## Methods

---

### Surface area change

COSMO Sky-Med satellite images were the basis of calving front position identification and of surface area change calculations, a satellite project funded by the Italian Ministry of Research and Ministry of Defense and conducted by the Italian Space Agency<sup>13</sup>. The images were obtained through personal communication with Anders Kusk (DTU Space, Denmark). The images have a fairly high, 5\*5 m tile resolution.

---

<sup>13</sup> <http://earth.esa.int/workshops/polinsar2003/participants/rum74/skymed.pdf>

Calving front positions were marked in QGIS when images were available, on 30.07., 07.08., 15.08., 23.08., 24.08., 27.08., 31.08. 2014. Once the calving fronts were marked, a polygon was drawn, its one side always adjusted to the position of the calving front on the respective day. In this manner, the area changes of these polygons were calculated between consecutive images. The resulting difference in surface area refers either to retreat, or to glacier advance, depending on the direction of change.

## Weather parameters

A range of atmospheric parameters are measured and recorded by automated weather stations at UI, that are operated by the PROMICE (Programme for Monitoring of the Greenland Ice Sheet) team, a collaboration between GEUS, DTU Space and Asiaq. There are two stations placed in the UI area. For this study, data from the station closest to UPE1 were obtained and analyzed. The location of the weather station is shown in *Figure 3*, the coordinates are: [72.8932, -54.2955]. The measuring height for air temperature was ca. 2.6 m above the ice surface. Air pressure refers to the barometric pressure in a logger enclosure. Cloud cover was estimated from down-coming long wave radiation and air temperature. Wind speed measurements were recorded at 3.1 m height from the ice surface. The ablation record represents a daily ablation estimate from depth pressure transducer data (typically drilled deeper than 10 m into the ice).

## Glacier velocity

For calculating glacier velocities, a complex and freely available image georectification and feature tracking MATLAB toolbox, ImGRAFT<sup>14</sup> (Messerli & Grinsted, 2015) has been applied. This toolbox combines post processing steps and utilizes DEMs and time-lapse photographs for feature tracking between pairs of images (in the same viewshed, using different timepoints). It can convert images from 2D to 3D and vice versa by projecting between pixel center coordinates and map coordinates, performing image georectification. ImGRAFT defines trackable features automatically and optimizes the camera view for each image. Since the camera at UI is set to take images in every thirty minutes, the time points are controlled. Given that the time difference between the examined images is known, once feature tracking is done, velocities can be calculated.

Beside the time-control on the frequency of shooting images, another great advantage of using time-lapse imagery is the high spatial resolution it provides on the calving front which is generally rather difficult to see on satellite imagery often used for monitoring the movement of glacier termini (e.g. Seale et al., 2011; Sugiyama et al., 2015).

The digital elevation model used in this study is the recently published (6. September 2017.) ArcticDEM<sup>15</sup>. ArcticDEM is a product of high-level computing and an open-source photogrammetry software applied on satellite imagery. In this analysis, the 2\*2 meter resolution version of the model

---

<sup>14</sup> <http://imgraft.glaciology.net/download>

<sup>15</sup> <https://www.pgc.umn.edu/data/arcticdem/>

was used that consists of overlapping DEMs with each DEM having a time and date registered to it<sup>16</sup>. To cover the glacier front area, a merged file of three ArcticDEM strips was applied, from 03.06.2014, 08.06.2014 and 28.08.2014 respectively. The DEM strip files are provided as 32-bit GeoTiff files that contain elevation data in meters. The majority of ArcticDEM data was generated from the panchromatic bands of the WorldView-1, WorldView-2, and WorldView-3 satellites. A small amount of data was also generated from the GeoEye-1 satellite sensor.

The time-lapse images used here are images that were taken under the program Extreme Ice Survey (EIS) led by James Balog<sup>17</sup>. There is a camera placed in Greenland, facing UPE1 ,capturing images of the glacier terminus. The location of the camera is: latitude: 73.00088889, longitude: -54.29102778. A sample time-lapse image recorded by the camera and used for feature tracking is shown in *Figure 6*.

---

<sup>16</sup> <https://eos.org/articles/map-provides-high-resolution-look-at-nearly-entire-arctic-region>

<sup>17</sup> <http://extremeicesurvey.org/about-eis/>



Figure 6.: Photograph of the calving front at UPE1, recorded by the EIS camera on 03. August 2014 at 14:40.

ImGRAFT projects georectified time-lapse photos onto the DEM so that feature displacements can be mapped. Unfortunately, the ArcticDEMs that cover UPE1 -and were merged later- are only available from 03. June, 08. June and 28. August 2014 respectively, and hence, the elevation models are not matching exactly the dates when the actual photographs were taken. Therefore, smoothing and filling algorithms were used to fill crevasses and séracs<sup>18</sup> in the merged DEM to make it correspond as much as possible to the surface that is captured by the camera. The smoothing has been done with a Gaussian spatial filter large enough to bridge the space between crevasses (Messerli & Grinsted, 2015).

---

<sup>18</sup> <https://pubs.usgs.gov/of/2004/1216/text.html#s>

To be able to track any feature movement, selecting reference points was necessary. These benchmarks are called Ground Control Points (GCPs), that are points outside the ice surface, preferably on the surrounding nunataks<sup>19</sup> or bigger rock surfaces. In this regard, the UPE1 glacier front's location is not ideal, as there are not so many exposed rock surfaces, and optimally the camera should sit at a higher elevation, ensuring a better, not so low view-angle. It is important to select the locations of these GCPs in a way that they can be identified both on the satellite and time-lapse images. For picking GCPs, an ASTER satellite image – received through personal communication with Karina Hansen (GEUS), image recorded on 28.08.2013., - was used due to its high optical resolution and for the convenience in data processing for it being in the same spatial reference system - EPSG:3413, WGS 84 / NSIDC Sea Ice Polar Stereographic North- as the rest of the data (ArcticDEMs, COSMO-SkyMed images, MEaSURES data). The reason for selecting this particular image was partly because this was available free of charge, as ASTER data are not accessible free of charge anymore<sup>20</sup>. Secondly, this image was opted for as it was taken in the same time of year (August) and the aim was to find an image closest possible in time to the month of August to have roughly similar snow and ice conditions as in August 2014. All in all, the effect of this offset in time is minimal, as the ASTER image was solely used for locating GCPs, marking distinguishable rock surface features which do not experience rapid changes in their location as opposed to ice.

---

<sup>19</sup> <https://www.britannica.com/science/nunatak>

<sup>20</sup> <https://earthexplorer.usgs.gov/>

First, GCPs were marked on the ASTER image with the help of a program called QGIS, a free and open source Geographic Information System<sup>21</sup>. Here, after the DEM that contained the elevation data was also loaded to QGIS, x, y and z coordinates were retrieved for each reference point. The x and y coordinates were given in meters in the EPSG:3413, WGS 84 projection in order to avoid distortion close to the pole. The z (elevation) values were obtained from the DEM *tif* file, in meters.

The u and v pixel coordinates of the GCPs, necessary for ImGRAFT to run, were derived from the time-lapse images in MATLAB.

Velocity values were retrieved from along a profile line where the fastest flow was expected, that extended from the calving front to 1292 m up-glacier from the front parallel to the flowline (Figure 15). The end coordinates of the profile are: [ -299349 -1828392; -300445 -1829089] and the investigated datapoints lie in every 25 m. One specific section was selected for in-depth analysis, at a distance of 372 m with respect to the glacier front, as this is the part where the strongest signal was expected. At < 370 m distances away from the calving front the available datapoints are sparse, and further away from this point the signal-to-noise ratio is expected to be much lower due to the difficulties the feature tracking algorithm faces at greater distances from the camera, given its view angle.

Time-lapse images are recorded on an hourly basis when there is daylight. In this report, one image per day was selected for analysis. The aim was to find images at about the same time of the day, every

---

<sup>21</sup> <https://www.qgis.org/en/site/>

day, when visibility was best with the least amount of fog, clouds or their shadows. It was not always possible to keep the 24 hours difference exactly, for instance when weather conditions were rough, or when there were issues with the SD card of the camera. In these instances, the image with an acceptable visibility nearest in time was chosen. The best timepoint proved to be at 14:40 each day. This allowed for having a controlled, ca. 24-hour gap between each image that were compared to one another. Consequently, the flow velocities discussed in this study are values derived from in-between two timepoints, between 14:40 every consecutive day, respectively.

## Results

---

### Surface area change

The difference between the surface areas at the calving front between 30.07.2014-31.08.2014. is ca. +0.0854 km<sup>2</sup>. The position-changes of the glacier front are depicted in *Figure 7/a*. It is shown in the figure that the most advanced position of the calving front was recorded on 27. August 2014. The most retreated front was observed on 30. July 2014. The area changes between the sample timepoints, representing ice loss or glacier advance at the front are given in *Table 1*.

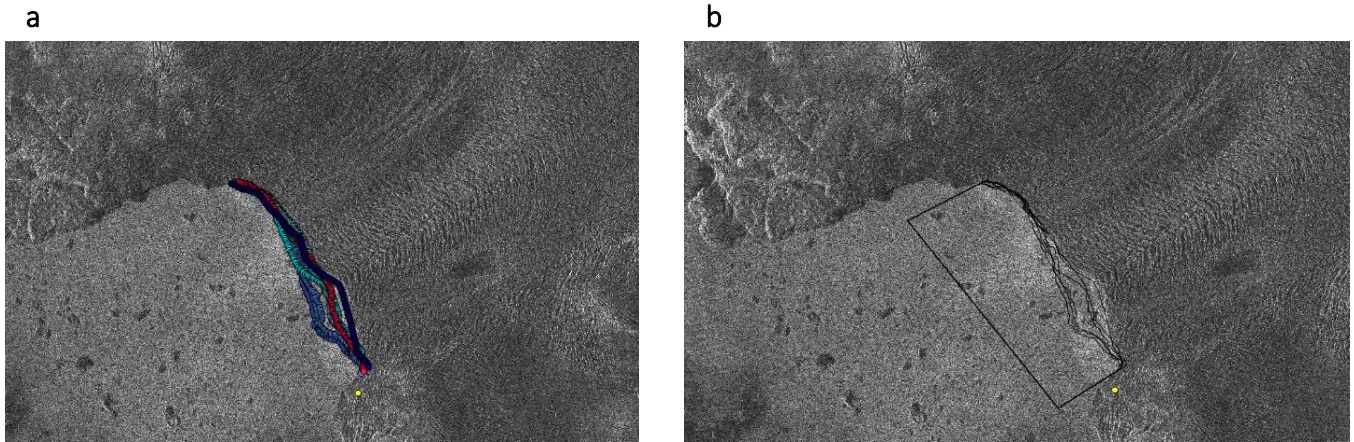


Figure 7.: COSMO SkyMED satellite image of the calving front at UPE1. Yellow dot shows the camera location. a): Calving front fluctuation over August 2014. The darkest blue line marks the calving front on 30.07.2014., the magenta colored line refers to the front position on 31.08.2014.; b): Surface area change in the same period, the polygon used for the calculations drawn in black.

Table 1.: Surface area changes at the calving front of UPE1 in August 2014. Positive value means more ice/ more advanced position of the front compared to previous timepoint. Negative value means retreat.

Date	Day to day (m)	Day to day (km <sup>2</sup> )
30.07.-07.08.	200066.3120	0.2001
07.08.-15.08.	-126406.8519	-0.1264
15.08.-23.08.	238310.5606	0.2383
23.08.-24.08.	-3189.3158	-0.0032
24.08.-27.08.	92396.2378	0.0924
27.08.-31.08.	-315802.8627	-0.3158

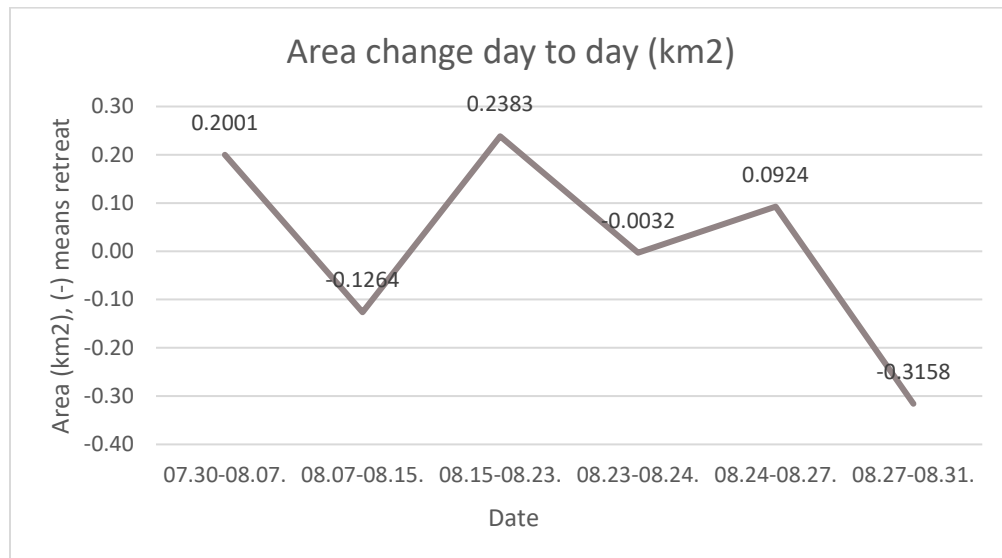


Figure 8.: Surface area change at the calving front of UPE1. Negative values represent retreat.

## Weather parameters

### Air temperature:

The average air temperature in August 2014 at UI was 4 °C. This is 1.5 °C below the reported<sup>22</sup> mean air temperature for August in the region.

<sup>22</sup> <https://en.climate-data.org/location/274141/>

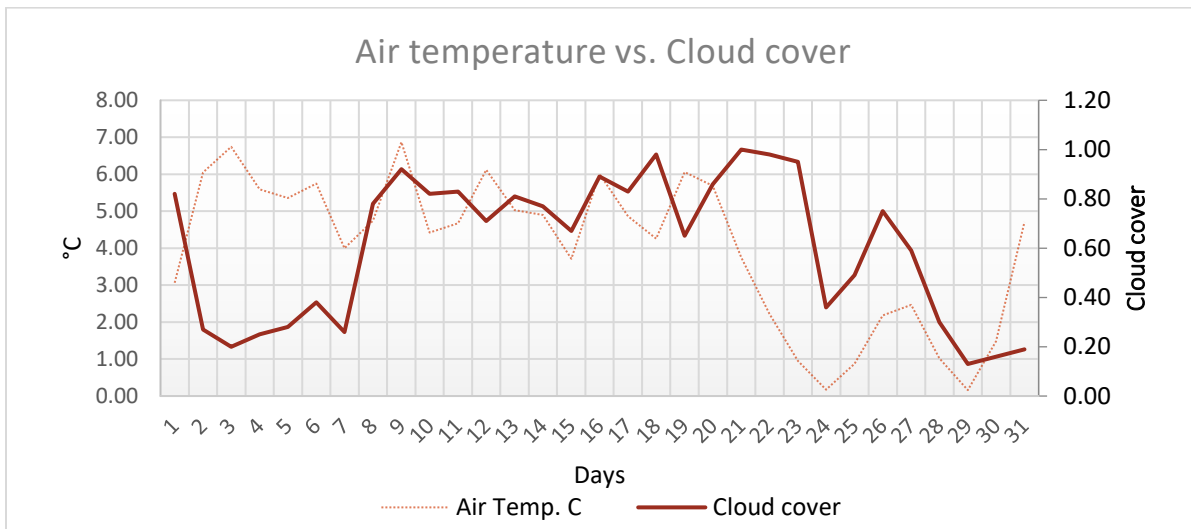


Figure 9.: Air temperature and cloud cover variation over August 2014 at UI.

Between 2 and 20. August, air temperatures fluctuated between ca. 4-7°C and dropped markedly after day 20, down to 0°C on 24. August. Thereafter the temperature only reached < 2.5°C until the very end of the month, when temperatures began to rise again up to ca. 3°C on 31<sup>st</sup> August.

The amount of cloud cover was greatest between 8-24. August with the least clouds in the beginning and the end of the month.

### Cloud cover:

Air temperature fluctuation over August showed only a weak correlation to changes in cloud cover ( $R=0.1488$ ,  $p=0.4243$ ) as depicted by *Figure 11/b*. In order to confirm a strong relationship between the variables at a significance level of 5%, a minimum correlation of  $R = 0.355$  should have been identified.

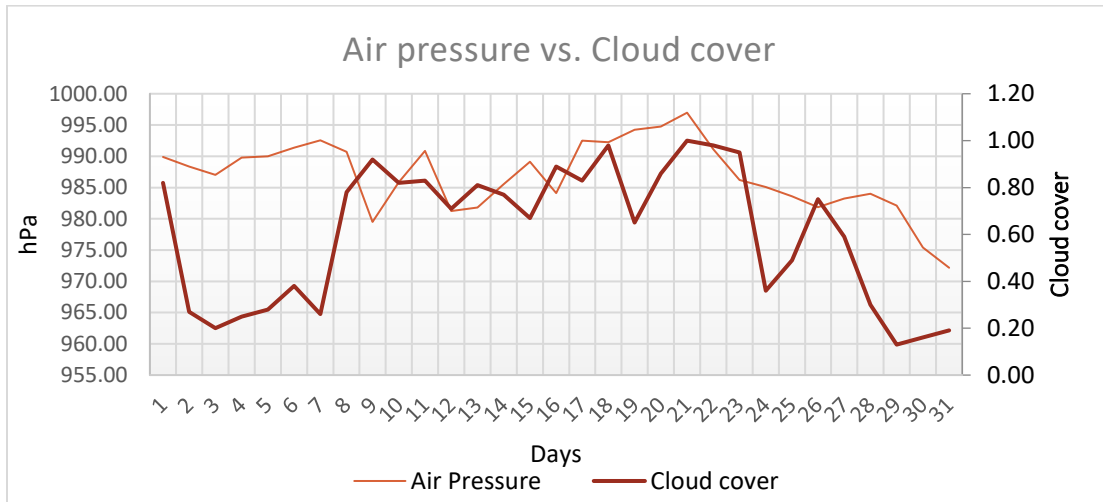


Figure 10.: Air pressure and cloud cover change over August 2014 at UI.

### Air pressure:

There is a stronger, although still only moderate relationship between observed air pressure and cloud cover ( $R = 0.3421$ ,  $p = 0.0596$ ) in August 2014, shown in *Figure 11/a*. Air pressure fluctuated between ca. 972-997 hPa (Figure 10.), the lowest pressures were measured towards the end of the month.

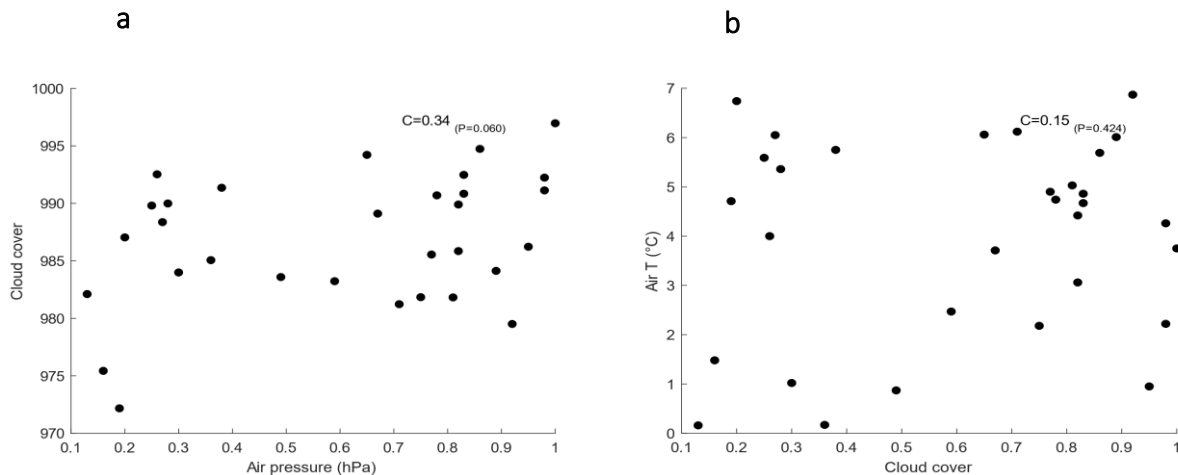


Figure 11.: a: Correlation between air pressure and cloud cover over August 2014 at UI. b: Correlation between air temperatures and cloud cover over August 2014 at UI.

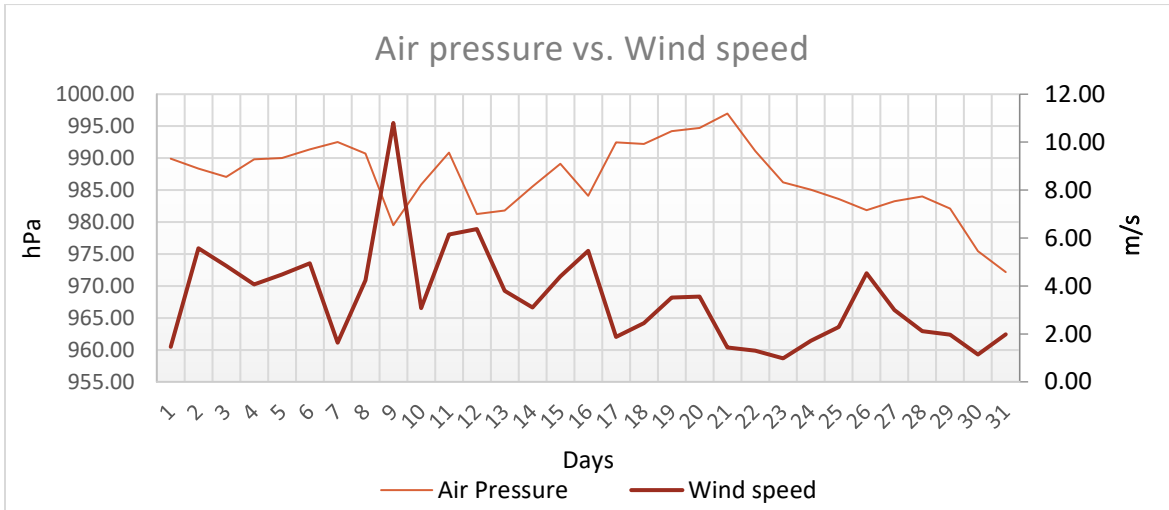


Figure 12.: Air pressure and wind speed variation over August 2014, at UI.

### Wind speed:

Wind speed was the highest on 9. August at ca. 11 m/s and fluctuated generally between 1-7 m/s over August. Low air pressures often coincided with elevated wind speed but that was not always the case.

A weak negative correlation of  $R = -0.1162$  ( $p = 0.5335$ ) was found between the two parameters with a high p-value that is indicative of the high level of chance in the statistics (Figure 12/a).

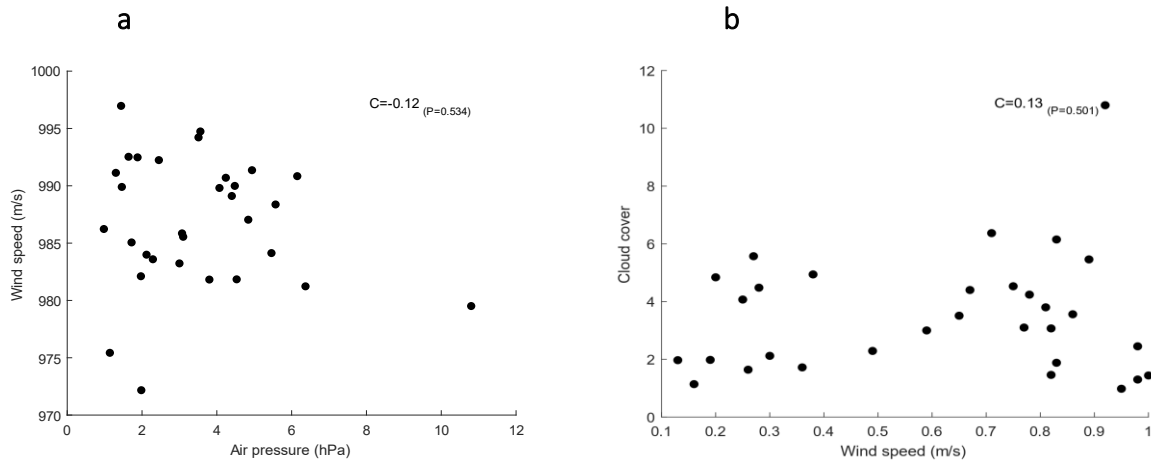


Figure 1.: a: Correlation between air pressure and wind speed over August 2014 at UI; b: Correlation between cloud cover and wind speed over August 2014 at UI. Sampling distance is ca. 370 m from the calving front.

After relating wind speed to cloud cover (Figure 12/b), a weak correlation was found between the two parameters ( $R = 0.1254$ ,  $p = 0.5015$ ).

### Other factors:

Ideally, other parameters such as precipitation, ocean water level and tidal fluctuations would have been investigated as well, but after reaching out to DMI (Danish Meteorological Institute) and DTU Space (Technical University of Denmark) it was confirmed that no stations were installed around Upernavik in 2014, therefore no local measurements are available that would allow for a high-resolution analysis. NOAA (National Oceanic and Atmospheric Administration) and EUMETSAT OSI-SAF (European Organization for the Exploitation of Meteorological Satellites - Ocean and Sea Ice - Satellite Application Facilities) provide publicly available data on sea temperature on a global scale, that is however not so relevant in this particular study as the focus is on changes within a very short time period at a specific location.

The weather station at UI recorded ice temperatures at different depths: at the surface, and in one-meter intervals from 1 m to 8 m depth. The biggest short-term variation in ice temperature would be expected to take place close to the surface, therefore data from the upmost section would have been of greatest interest for this study. Unfortunately, it seems that the ice has melted from around the sensors, and temperatures so high as +4°C were measured at a (theoretical) 2 m depth. (Plots are found in the appendix.) Therefore, these data were considered unreliable and were not used for further analysis.

## Calving events

Days with calving events were noted based on visual inspection of the time-lapse images. There were 11 days in August 2014 (day 4, 5, 9, 10, 11, 14, 17, 20, 28, 29, 31) where calving was captured by the camera, four events out of these were massive. Calving days are shown in *Table 2* along with days when velocities greater than the mean monthly value were observed at ca. 370 m distance from the calving front and when air temperatures were exceptionally high, over 6°C.

Faster flow than the mean was observed on 12 days at ca. 370 m distance from the calving front. There were two days (16., 27. August), when faster than average flow was followed by calving on consecutive days, and six days (05., 9-11., 14., 20. August) when greater than average flow speed coincided with days with recorded calving. On three occasions (06., 12., 21. August), higher than average velocities were observed on days immediately following days with calving. One day (22. August) with relatively fast flow neither preceded nor followed a day when the glacier calved.

Further investigating the relationship between calving events and flow velocities at ca. 370 m from the calving front, it is shown in *Figure 13.*, that flow was in general faster on days with calving than on days without calving events. Half the times when calving was recorded, daily mean velocities were between ca. 20 m/day and 70 m/day and the median value was ca. 44 m/day. On no-event days the median speed was ca. 37 m/day and 75 % of the daily mean velocities were found to be below ca. 56 m/day. The range of velocities was however greater on days without calving.

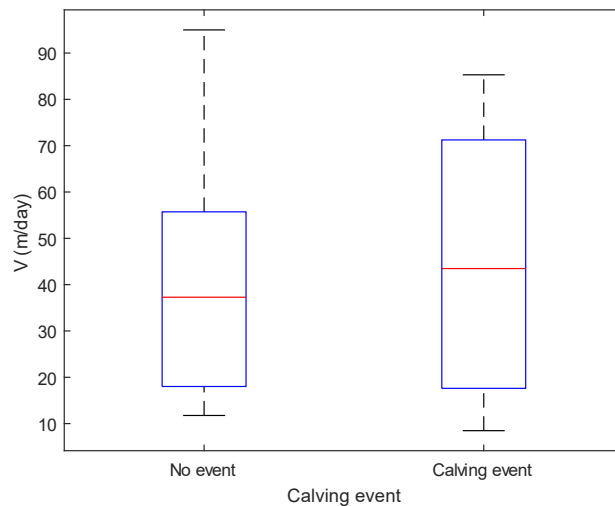


Figure 2.: Boxplot showing the relationship between calving events and flow velocities at ca. 370 m away from the calving front of UPE1.

In order to investigate any possible links between calving events and air temperature variation, exceptionally warm days with daily mean air temperatures over +6°C were also listed in *Table 2.* Altogether six days were warmer than +6°C in the discussed period. On three occasions (03., 16., 19. August) warmer than average days preceded days with calving events. One warm day (09. August)

coincided with, and one (12. August) followed a day when the glacier calved. One day (02. August) with  $> +6^{\circ}\text{C}$  mean daily temperature was neither immediately before or after, nor on the same day as when the glacier calved.

Table 2. First column: Big calving events in August 2014 at UPE1, days with the largest calving events are in bold. Second column: Peak air temperatures in August,  $T > +6^{\circ}\text{C}$ . Third column: Velocities greater than the mean at 372 m from the glacier front along the velocity profile.

Colors: light blue: Days with calving; orange: a day with high air temperature/high velocities was followed by a day with calving; red: calving occurred on the same day with elevated air temperatures/high velocities; dark blue: high air temperatures/velocities after a day with calving; green: warm/high velocity day neither immediately before nor on the same day as calving.

Calving	Air $T > 6^{\circ}\text{C}$	$v > \text{mean}$ at 372 m
2014 August		
Day number		
1	1	
2	2	2
3	3	3
4	4	4
5	5	5
6	6	6
7	7	7
8	8	8
<b>9</b>	9	9
10	10	10
11	11	11
12	12	12
13	13	13
<b>14</b>	14	14
15	15	15
16	16	16
17	17	17
18	18	18
19	19	19
20	20	20
21	21	21
22	22	22
23	23	23
24	24	24
25	25	25
26	26	26
27	27	27
<b>28</b>	28	28
<b>29</b>	29	29
30	30	30
31	31	

## Glacier velocity

After running ImGRAFT, the feature tracking tool, feature displacements on the surface of UPE1 in the EIS images on consecutive days were converted into 'real' movements (in meters). This is illustrated in *Figure 14.*, where the red arrows show the direction and magnitude of displacements between two timepoints, at 14:40 on 10. and 11. August 2014., 24 hours in-between. Many red arrows are seen at the south-eastern part of the glacier terminus, this is where most of the motion was concentrated at. Calving events were recorded by the camera on both days, and the velocities were greater than average on both 10. and 11. August. Red arrows above the rock where the camera stands are most likely due to an error in the ArcticDEMs, which tend to amplify any minor horizontal movement near the camera. DEMs are often inaccurate where glacier-ice is present, as the ice is constantly on the move. Furthermore, the DEM used in the analysis was merged from three individual DEMs dated to different days that can cause inaccuracy.

Red arrows west from the calving front represent sea-ice movement which is not further discussed in this study.

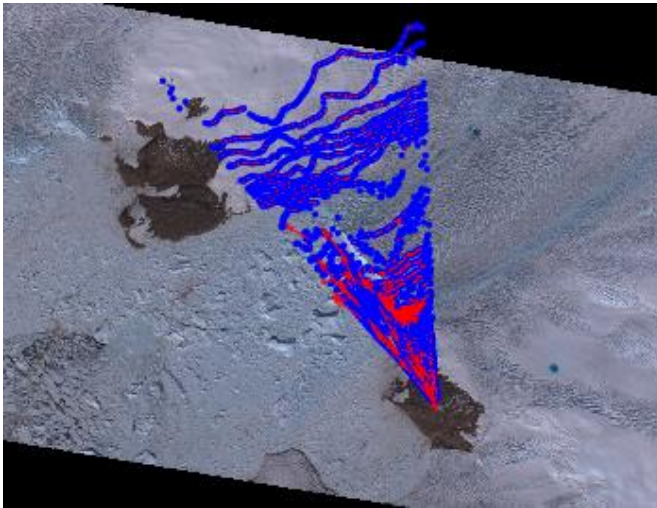


Figure 3.: ASTER satellite image of UPE1. The area where the blue marks are concentrated indicate the camera view field. The actual positions of the blue marks show where ImGRAFT tracked features in a pixel-based grid between 10-11. August. Red arrows refer to pixel movements from one day to the next, that are converted to real life movements in meters.

Glacier flow speed was calculated for each day of August 2014, along a ca. 1300 m long line parallel to and within the flow line (Figure 15/b).

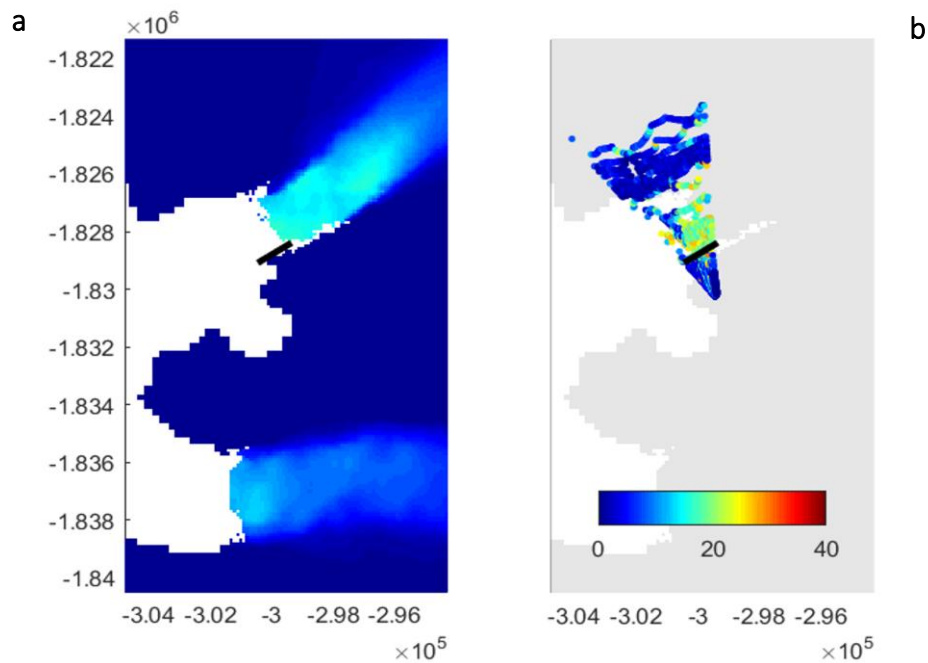


Figure 4.: a): Velocity map based on NASA's Making Earth System Data Records for Use in Research Environments (MEdSUREs) data. The values indicate the mean velocity between 22. August- 02. September 2014. b): Velocity map based on time-lapse imagery feature tracking between 10-11. August 2014., images taken at 14:40 both days. Thick black line indicates the location of the profile line at UPE1. Colorbar refers to velocities in m/day. Axis tickmarks represent northings and eastings.

*Figure 15/a and b* illustrate glacier velocities at UPE1 along the velocity profile line. *Figure 15/a* represents velocities inferred from NASA's MEaSUREs program (Joughin et al. 2010), based on TerraSAR-X imagery. Velocities shown in the figure are mean velocities between 22. August- 02. September 2014. In *Figure 15/a*, velocities were only available and therefore are only displayed further inland from the profile line's end, with values reaching ca. 20 m/day. This lack of data is probably due to the characteristics of the satellite. TerraSAR-X does not perform well in wet areas, e.g. where there is water at the surface of the glacier which is not uncommon in the melt season near the front. In such regions, only a small or no signal returns to the satellite sensor. The TerraSAR-X velocity map was derived using intensity offset tracking, that can further limit its applicability close to the calving front of a glacier, as the tracking tends to fail when the surface had changed too much between two images that were compared to each other which is often the case at glacier fronts. In light of the above, land-based, optical imagery such as the EIS photographs can be an excellent tool to complement data from satellite images.

*Figure 15/b* shows velocities attained after applying the feature tracking algorithm on the EIS time-lapse images between 10-11. August 2014. at 14:40 both days. As seen in *Figure 16.*, velocities are greatest at that segment of the profile which is closer to the glacier terminus. Lack of data is represented by blank areas in *Figure 16.*, and they are blank either because the extremely low velocities were filtered out by the feature tracking algorithm, or because the algorithm could not track anything on certain days due to weather conditions e.g. fog or the presence of clouds and their shadows on the ice. The pixel-size in the y direction of the plot translates to 12.5 m. At some parts of the profile, negative velocities were found by ImGRAFT, which were disregarded in the analysis. Negative velocities occur when the

direction of flow changes to the opposite direction. In the case of a glacier this would mean an upstream flow, which may locally occur if a specific feature -typically crevasses- had moved away from the glacier front towards the mainland. Such phenomenon can occur if ice pushes in from the margins of the glacier (or from the sides of the analyzed flow line) to the front of the feature, pushing the ice mass -where the tracked feature is located- further up-stream. However, the investigated profile line covers only a thin section of the glacier flow line, the velocity results shown here are strictly specific to those particular sections. Therefore, any locally found indications for upstream flow would not necessarily affect any other parts of the glacier. Alternatively, negative velocities might also be a result of a failure in feature tracking.

Close to the glacier front, up to ca. 500 m away from the front, glacier velocities were greatest with respect to the entire profile section. The highest values reached 95 m/day at ca. 370 m away from the front, and the mean velocity was 25.53 m/day. The ca. 370 m distance is the segment of the profile that was thoroughly investigated in this thesis, as it is here we expect the best quality data from the feature tracking. At shorter distances there are not so many datapoints available and further inland from here the ratio of noise in the data is likely higher. Velocities at ca. 370 m from the glacier front (Figure 16.) varied between 8.47-95 m/day, 45.63 m/day was the mean velocity and the median was 41.88 m/day.

At a distance of ca. 500-1080 m from the front there are data available for almost every day of the month. In this section, the majority of the datapoints represent velocities below 20 m/day, with lower values more upstream and higher values closer to the glacier front, adding up to a mean velocity of 15.69 m/day. Data > 1080 m were untrusted and thus filtered out due to the blurriness of the EIS images

so far from the camera, making the feature tracking fail at such distances. Consequently, there are no velocity values calculated in this section of the profile.

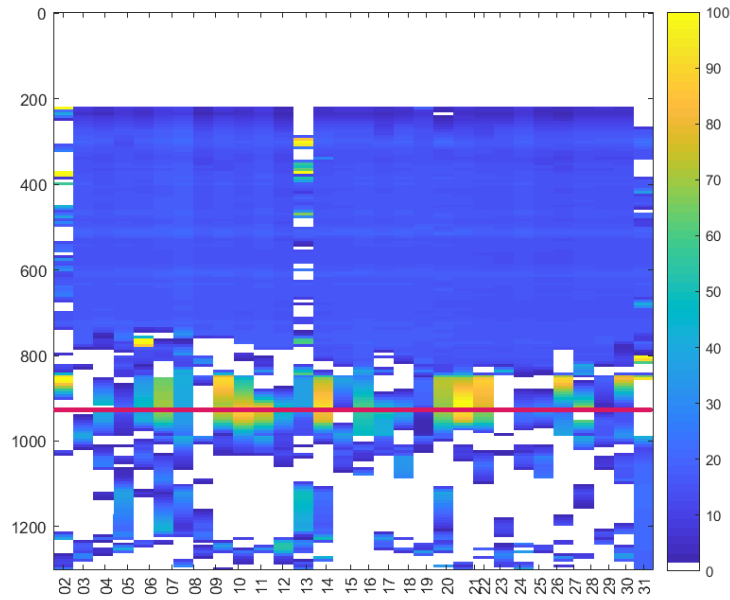


Figure 5.: Calendar plot showing the velocities along the profile line on each calendar day of August 2014 (x axis) at UPE1. Y axis shows the distance [meter] from the glacier front (glacier front 'lies' at the bottom of the figure, parallel to the x axis). The dark red line marks the 25 m long section at ca. 370 m away from the calving front, where velocities were more closely analyzed. Colorbar denotes velocity values [m/day].

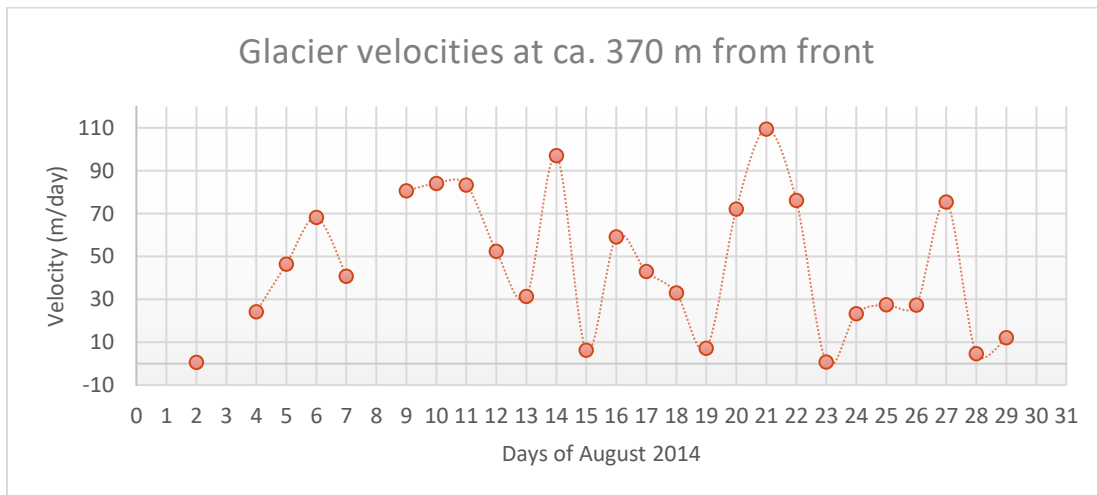


Figure 6.: Flow velocity fluctuations of the UPE1 glacier between 1-30. August 2014, ca. 370 m away from the calving front. Values are missing when there was a gap in the velocity dataset.

*Figure 17.* provides a clearer visualization of the velocity fluctuation from one day to the next, at the same part of the glacier, ca. 370 m away from the calving front. The fastest flow (95 m/day) was observed between 20-21. August, the slowest (0.65 m/day) between the first and the second of August. Similarly, low velocities were found between 14-15., 18-19., 22-23. and 27-28. August. Velocities grew by up to ca. 65 m/day during ca. 24 hours between 13-14. August and dropped by maximum ca. 90 m/day from 14. to 15. August. The second largest velocity difference between consecutive days were observed between 19-20. August, the flow speed growing by 63 m/day and dropping by 75 m/day between 22-23. August. The least changes between consecutive days ( $dv < 4.2$  m/day) were recorded between 09-11. and 24-26. August.

Day-pairs with the fastest speedups were between 13-14., 15-16., 19-20., 26-27. August. The greatest velocity drops took place between 14-15., 22-23, 27-28. August. With respect to calving events, the pattern is less clear than in the case of speed-ups. The drop between 14-15. August occurred after a calving event on 14. August, and the recorded calving on day 28 preceded the drop between 27-28. August. The third velocity drop between 22-23. August occurred neither on a day immediately before nor directly after calving.

## Relationship between weather parameters and glacier velocity

With respect to glacier flow variations on a short timescale and their possible causes, one of the most important atmospheric parameters to look at is air temperature, which is found to directly influence ablation (Cuffey and Paterson, 2010). This positive relationship between air temperatures and ablation was confirmed by weather station measurements at UI (Figure 18). With a significance level ( $\alpha$ ) of 0.05,

and a degree of freedom of 29 (and the Pearson correlation coefficient (R) being greater than 0.355)<sup>23</sup>, a statistically significant relationship (R = 0.64) was found between ablation and air temperatures. This result would occur 1/1000 of the times tested, based on true randomization with  $p = 0.0001$ .

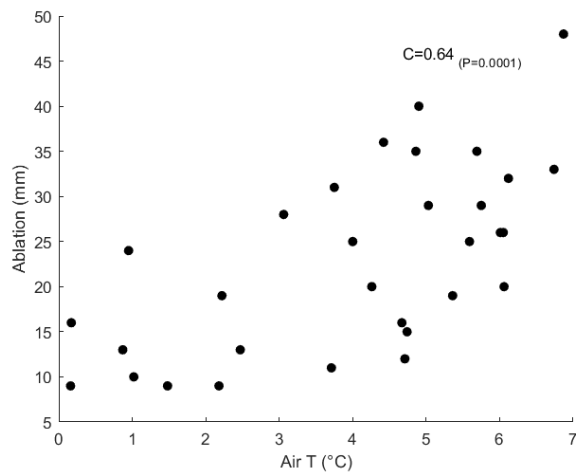


Figure 7.: Correlation between air temperature and ablation at ca. 370 m from the calving front.

Figure 19. shows air temperature and ablation variations in a daily breakdown over August 2014 for better visualization. The temperature and ablation values are daily averages calculated from hourly recorded data. In the first half of the month the amount of ablation followed the air temperature changes relatively well. However, at the end of the month this pattern changed, and the amount of ice lost was not following air temperature changes very closely.

<sup>23</sup> [https://researchbasics.education.uconn.edu/r\\_critical\\_value\\_table/](https://researchbasics.education.uconn.edu/r_critical_value_table/)

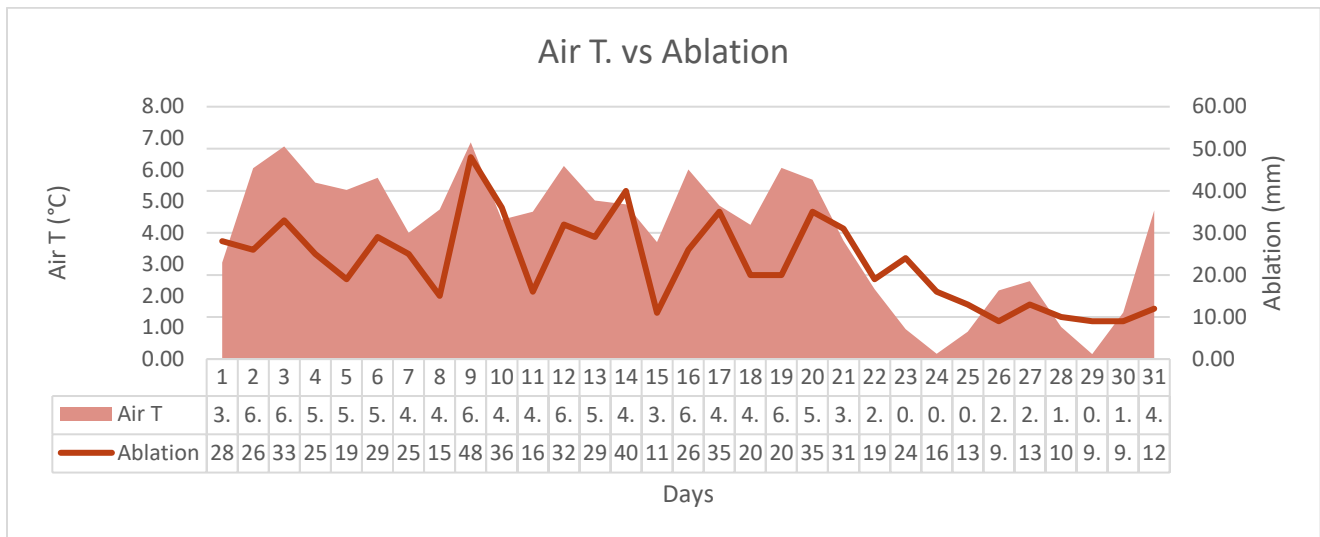


Figure 8.: Air temperature and ablation variations between 1-31. August 2014 at UI.

In order to understand glacier flow velocity fluctuation, it is also important to look at how ablation (and thus, indirectly, all the above-mentioned parameters) may influence the flow speed of ice.

As suggested by several authors (Joughin et al., 2008; A. V. Sundal et al., 2011; Van De Wal et al., 2008) surface melting (a key ablation process) influences glacier speed. In order to see how ablation and glacier velocity relate to each other, their relationship was tested. Having 29 samples, it can be established with a fail rate of 5% ( $\alpha = 0.05$ ) that there is a positive correlation ( $R = 0.4588$ ,  $p = 0.0123$ ) between ablation and glacier velocity at ca. 370m distance from the glacier front.

The relationship between day-to-day changes in velocity and ablation was also tested. With a certainty of 5 in a 100, the Pearson correlation coefficient over 0.55 ( $R = 0.5576$ ) and a p-value of 0.0021, a strong positive correlation was found between the day-to-day velocity and ablation changes. One in 476 randomizations would lead to at least this high correlation level.

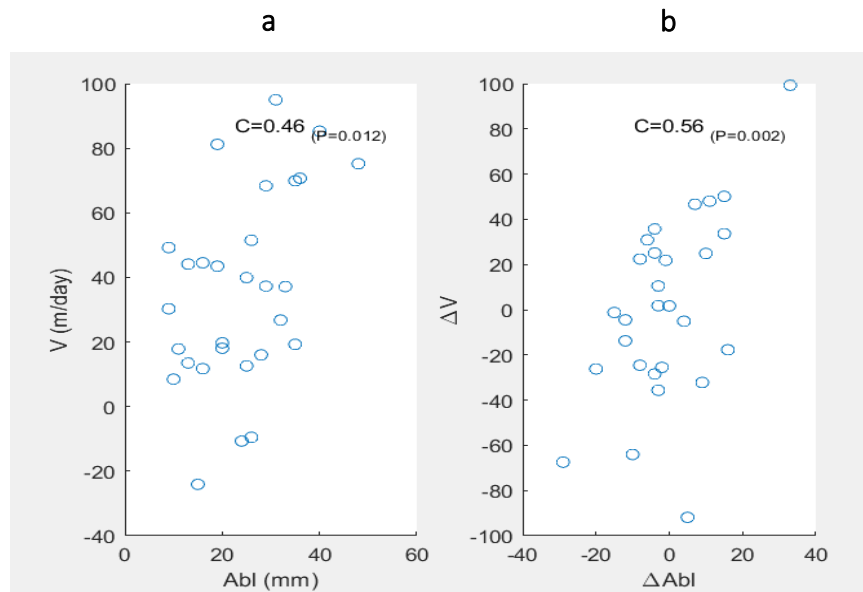


Figure 9.: a): Correlation between ablation and glacier velocity; b): Correlation between ablation change and velocity change on a day-to-day basis. Ablation measurements taken at the PROMICE weather station, velocity changes were examined ca. 370 m more inland from the calving front at UPE1, over August 2014.

## Discussion

---

Tidewater glaciers showed widespread velocity acceleration in the past decades and the increased flow is expected to continue in the forthcoming years (Rignot et al., 2011).

In order to gain more understanding of the processes influencing glacier flow speed, several weather parameters measured at UI over August 2014 were analyzed and related to flow velocity changes close to the glacier front. Surface area variation that resulted from these interactions near the glacier front were also investigated.

## Surface area change

A surface area change of  $+0.0854 \text{ km}^2$  was observed at the calving front of UPE1 between 30.07.2014-31.08.2014. The most advanced position of the calving front was recorded on 27. August, the most retreated front was observed on 30. July. Unfortunately, COSMO-SkyMed images were only available on a limited number of days within the focus period, making the attempt to investigate the relationship between calving events and calving front position change challenging. There is one day in the satellite image record, the 27. August (with the most advanced front line in the month), which was followed by a day with recorded calving. Velocities were found to be above average on 27. August, the day before calving. In the next available satellite image (31. August) the calving front was markedly retreated, that may be the result of the calving event on 28. August.

## Weather parameters

*Figure 21.* depicts a strong correlation between positive degree days and ablation during summer (Cuffey and Paterson, 2010). The more days with temperatures above  $0 \text{ }^\circ\text{C}$ , the greater was the ablation at several glaciers in Greenland.

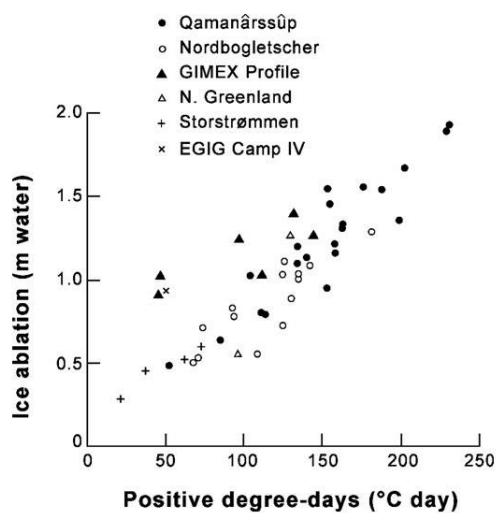


Figure 10.: Correlation between positive degree days and ice ablation (from Cuffey and Paterson, 2010)

Prior work has suggested however (Hofer et al., 2017) that instead of rising air temperatures being the key source of melt increase in Greenland- as suggested by *Tedesco et al., 2013*, it is likely linked to reduced cloud cover in the summer and can be attributed to a combination of greater short wave downward radiation and an increase in long wave downward radiation (that is dependent on the greenhouse gas content of the atmosphere (Wang & Dickinson, 2013)).

Based on the weather station measurements at UI, there was only a weak relationship ( $R = 0.15$ ) identified between air temperature and cloud cover. Where cloud is present in the atmosphere, they can have either a heating or a cooling effect on the Earth's surface, depending on many factors, e.g. the given cloud's size, altitude and its constituents. They can absorb and/or reflect and reemit radiation of certain wavelengths<sup>24</sup> As reported by *Van Tricht et al., 2015*, clouds reduce annual mean surface

<sup>24</sup> <https://earthobservatory.nasa.gov/Features/Clouds>

radiative heat loss as they control the emitted long wave radiation and thus have a positive feedback on melt rates. The authors also showed that clouds enhanced meltwater runoff by about one-third relative to clear skies. According to *Hofer et al., 2017*, decreasing summer cloud cover tends to increase the melt-albedo feedback as the reduced amount of clouds let more of the incoming radiation in the atmosphere. Other studies suggested that the increase in melt can enhance the melt water runoff supply, potentially lubricating the glacier bed and promote glacier flow (Schellenberger et al., 2015).

Given the above proposals, the weak correlation our data showed between air temperature and cloud cover seems lower than what was expected. We can speculate that since our data is focused on only a month's period, the results might be different from results derived from greater datasets investigating longer periods. It is also possible that in August 2014 a certain type of clouds dominated the area containing a certain type of constituents that might not be representative elsewhere or on the longer run. In relation to the amount of clouds present in the area, *Hofer et al., 2017* linked the decreasing cloud cover to large-scale climatic variations, as shifts in the North Atlantic Oscillation (surface sea-level pressure difference between the Subtropical -Azores- High and the Subpolar Low<sup>25</sup>).

With respect to cloud cover and wind speed, the weather station data analysis resulted in a similarly low correlation value ( $R = 0.13$ ) between these parameters. Air movement can promote cloud formation by carrying water droplets and aerosols and can also influence the shape and position of clouds<sup>26</sup>, thereby affecting the role of the cloud on radiation and possibly on ice melting.

---

<sup>25</sup> <https://www.ncdc.noaa.gov/teleconnections/nao/>

<sup>26</sup> [https://www.nasa.gov/pdf/135641main\\_clouds\\_trifold21.pdf](https://www.nasa.gov/pdf/135641main_clouds_trifold21.pdf)

Regarding the relationship between air pressure and cloud cover, our data showed a moderate correlation ( $R = 0.34$ ) between these variables in the focus period. Air pressure can potentially be a good indicator for windspeed- which is closely linked to wind deflation, an important ablation process- as wind occurs due to differences in atmospheric pressures.<sup>27</sup> However, after correlating wind speed and air pressure, only a weak negative relationship ( $R = -0.12$ ) was found between these factors. This is at odds with the expectations, a stronger negative correlation value, but aligns well with the similarly weak correlation between wind speed and cloud cover.

## Glacier velocity

Beyond the distance of ca. 500 m up to ca. 1080 m away from the glacier front- the limit of our dataset on the inland side- along the velocity profile at UPE1, the mean velocity was calculated (after feature tracking) to be at 15.69 m/day (5.73 km/yr). *Larsen et al., 2016* presented flow velocities around 6.5 km/yr at a ca. 3 km distance from the calving front of UPE1 and approximately 5.6 km/yr flow speed at a ca. 6.5 km distance from the front of the glacier in 2007. Year 2007 however, was in the middle of an accelerating period, the near terminus velocities grew by ca. 50-60% (2 km/yr) between 2006-2008, and the acceleration reached distances over 20 km inland. The authors also report that the maximum flow speed (within the test period between 1992 - 2013) was found in 2011, and the high velocity levels remained in 2012-2013, until the end of the sample period.

---

<sup>27</sup> <https://www.metoffice.gov.uk/learning/wind>

Comparable flow speeds were found by *Rignot and Mouginot, 2012* for fast-moving glaciers in the north-west and center-west parts of Greenland - where UI is located as well-, with flow velocities at 4.2 km/yr for Rink Isbræ, 3.1 km/yr for Sermeq Kujalleq and 3.7 km/yr for Store Glacier. It is worth noting that these velocities were identified referring to the entire glaciers, respectively, taking into account the slower, far-inland parts of the glaciers as well, that was excluded from this study. Velocities generally decline towards the point of origin of the glacier (*Larsen et al., 2016*), and thus, even though the velocity values derived from the EIS images close to the calving front are higher than the before-mentioned velocities referring to the full-lengths of other Greenland glaciers, they can be well in alignment had they been complemented with additional data from further up-glacier. For putting the above into perspective, at another branch of UI, UPE3, *Ahlstrøm et al., 2013* identified summer glacier velocities of ca. 0.6-1 km/yr at a distance of 41.5 km upstream between 2009-2012. Directly transposing these findings to UPE1 however is advised against, as the separate branches of the same ice stream can behave markedly different (*Ahlstrøm et al., 2013; Larsen et al., 2016; Moon et al., 2012a*).

The significant seasonality (e.g. *Ahlstrøm et al., 2013; Lemos et al., 2018*) in glacier flow is also a factor to take into account when discussing yearly velocities. *Ahlstrøm et al., 2013* found glacier flow velocities in north, west and south Greenland to peak in the early melt season, that is followed by a mid-melt season deceleration, the seasonal variations being most notable near the glacier terminus. The authors also reported that the pattern of seasonal velocity variation seems to be specific to each glacier with a tendency to reproduce the same pattern in succeeding years. It has been proposed that the seasonal speed-change is largely controlled by changes in basal traction and is induced by surface meltwater penetration to the glacier bed (*Lemos et al., 2018; Sundal et al., 2011*). Interestingly, *Sundal et al., 2011*

observed a summer speed-up drop of the GrIS in high melt years as opposed to low melt years during a five-year-long period and reported generally slower and shorter periods of increased flow in the summer during warmer years.

The ImGRAFT-inferred mean velocity of 5.73 km/yr at distances over ca. 1080 m is in agreement with the MEaSURES- derived velocities further inland that were ranging between 15-20 m/day, corresponding to 5.46-7.3 km/yr. When comparing the results from feature-tracking and satellite-inferred velocities, some deviance is likely to occur on account of the different data obtaining and deriving methods, based on the results of *Ahlstrøm et al., 2013*, who found a mean velocity difference of 9.5% between TerraSAR-X satellite-derived and in-situ GPS velocity measurements. One should also bear in mind that the reliability of the ImGRAFT-produced velocity values in this distant section of the profile is beyond optimal.

Based on the results of feature-tracking in the time-lapse images, the fastest flowing section of UPE1 was identified between 0 m (the glacier front) and 500 m, with a mean velocity value of 25.53 m/day. Further analysis of flow speed was carried out on the basis of results from one short segment of this section, recorded at ca. 370 m inland from the glacier front. This is the section of the profile where a sufficient amount of datapoints were identified by ImGRAFT and where the noise in the data was relatively low compared to further inland sections. At this distance, the flow speed fluctuated notably (ca. between 0-110 m/day) over the whole month of August. The largest speed-ups were in each instance observed before days when calving was recorded. In the case of velocity-drops no such pattern could be observed.

## Ablation and glacier velocity

In August 2014, calving events were recorded by the EIS camera on eleven days (04., 05., 9-11., 14., 17., 20., 28., 29., 31. August). Four events out of these were massive.

8 days out of 11 with velocities greater than the mean were observed either on the same day as when the glacier calved, or just before those days. Velocities in general were found to be higher on days with calving than on no-event days, with a higher median velocity as well. This is in alignment with previous expectations, as calving and increased flow often coincide (e.g. Khan et al., 2013; Moon et al., 2012; Pimentel et al., 2017). In fact, the time-lag between ablation and velocity change can be so short as a few hours in the summer, from July on (Müller and Iken 1963).

Tidewater glacier retreat can be caused by calving or submarine melt (Haubner et al., 2018), and as shown by *Benn et al., 2007*, calving rates can increase markedly as a response to flow acceleration.

Results of this study showed that faster than average flow was observed on three days that followed days when calving was recorded. Considering the rapid loss of enormous ice volumes at the front during calving, it is likely for such events to have a positive feedback on the more inland parts of the glacier, resulting in increased velocities after calving (Sundal et al., 2013). *Nick et al., 2012* highlighted that acceleration and thinning occurs all along the flowline of a glacier, although it is a widely accepted view that they are initiated at the glacier front. However, the relationship between calving and acceleration seems to be rather complex, as *Lemos et al., 2017* found calving front advance during melt season speed-up at the north-Greenlandic Petermann Glacier and concluded that ice front retreat does not coincide with seasonal flow acceleration. It has also been reported that at the western margin of the

GrIS, annually averaged velocities decorrelated the annual mass balance between 1991-2008 (Van De Wal et al., 2008).

After relating the calving events to elevated air temperatures at UI, it was found that days warmer than +6°C preceded days when calving was recorded three times (50% of all > +6°C days) over the month of August. In addition to these warm days, there were three more days in August with higher mean daily temperatures than +6°C, one immediately before, one immediately after a day with calving and one coincided with glacier calving. These results are in accordance with previous findings, namely that terminus retreat at UI were associated with elevated air temperatures in multiple time periods (Andresen et al., 2014). The amount of water present in crevasses was also found to play an important role in terms of calving events (Cook et al., 2012). A few meters change of water level in near-terminus crevasses, that is directly linked to surface melt water availability, can cause a shift from glacier advance and retreat (Otero et al., 2017).

*Cuffey and Paterson, 2010* claims that positive degree days, hence air temperature is a better proxy for ablation than expected from the physics behind: Empirical values lie around 8 mm of ablation for each 1 °C warming, however models would predict 4-6 mm of ice per day for the same warming. The difference may originate from the complexity of factors influencing ablation rate. It has been a clear pattern however, that positive degree days were in favor of enhanced ablation at multiple glaciers in Greenland.

High air temperatures can cause the ice to melt, increase the melt water runoff supply (Sundal et al., 2013) which in turn can promote hydro-fracturing crevasses near the calving front that are filled with

water (Joughin et al., 2008) or percolate down to the base of the glacier, lubricate the bed and thereby accelerate the flow (Schellenberger et al., 2015; Van De Wal et al., 2008). *Zwally et al., 2002* argued in favor of this theory and suggested that rapid migration of melt water from the surface down to the ice-rock boundary positively affects glacial sliding. Other authors concluded that flow velocities are responsive to changes in the ablation rate solely on a short, weekly time scale, and instead of the absolute amount of melt water present, the change in melt water availability is the key factor for determining the velocity fluctuation within a season (Van De Wal et al., 2008). Consequently, a long-term increase in melting can result in a decrease in flow speed. In this fashion, as the positive relationship between melt rate and flow speed is likely to be a seasonal process, it may not be determinative in terms of ice sheet response to large-scale climate change as discussed above. A previous study reported a relatively low, 10-15% contribution from melt-induced acceleration to recent glacier speedups, and suggested that internal dynamics are the main cause of flow acceleration (Joughin et al., 2008).

From the ImGRAFT-derived data a positive correlation was found both between ablation and glacier velocity ( $R = 0.46$ ), and between ablation-rate and glacier velocity change ( $R = 0.56$ ), the latter demonstrating a stronger relationship. This indicates that glacier flow speed change and the rate of ice loss by ablation, processes such as calving and melting are interconnected. However, since the correlation is far from perfect, it is not a simple relationship between these parameters, other factors also play a role in ablation and velocity fluctuation over time.

The strong relationship found between ablation change and velocity change seems to fit well with the results of a study by *Van De Wal et al., 2008*, namely that it is the change in ablation that promotes

flow velocity variation rather than the absolute available amount of meltwater, and that flow speed only reacts to ablation rate change on a weekly time-scale. Although, this thesis only covers a time-period of a few weeks, therefore there were no data analyzed outside this period.

*Truffer et al., 2010* hypothesized that a developed water drainage network can divert subglacial discharge into a few big channels in high-runoff periods, thereby reducing basal motion that can often be observed towards the end of the melt season (Ahlstrøm et al., 2013), when flow velocities are relatively low in spite of high water discharge. Hence, it is likely, that increased melting does not necessary lead to proportionate increases in flow speed (Sundal et al., 2011), and developed internal drainage systems may adjust to the enhanced melt water input, maintaining annual velocities relatively stable (Van De Wal et al., 2008). Such records highlight the complexity of the meltwater-basal motion relationship and warn against the possible over-simplification of processes as suggested by *Zwally et al., 2002*.

## Role of sea

Another important factor to consider in terms of ice loss, thinning, and thereby the acceleration of glaciers is the role of sea-water (e.g. Sugiyama et al. 2015; Straneo and Heimbach, 2013). In this report, the effect of fjord-water on glaciers was not investigated due to the fact that there is no measuring station installed in the vicinity of the UPE1, that could have provided high-resolution and region-specific data with respect to water level and tidal motion for further analysis. Nonetheless, it is essential to mention the relevance of ocean water when discussing glacier dynamics.

Although grounded glaciers -such as UPE1, grounded since 2013 (Larsen et al., 2016)- are less affected by the contact with sea as less ice surface is being exposed to the ocean than at glaciers with a floating tongue, their influence on glacier dynamics is far from negligible. In case of UPE1, the calving front was ca. 1 km thick in 2013 (Larsen et al., 2016), the grounding line depth was between 400-700 m (Morlighem et al., 2014), and hence the ice-surface being in contact with the sea was significant. This contact is important given the thermal stratification of water in the fjord. There is relatively low salinity, warm water (< ca. 2.2°C) present in the topmost, ca. 50 m thick water- layer followed by a temperature drop between ca. 50-150 m depths, where temperatures only reach 0.5-1.5 °C. Towards the bottom of the fjord, temperatures gradually increase again from ca. 1.5°C to 3°C and the water becomes more saline (Andresen et al., 2014). This relatively warm water can melt the glacier where they come into contact, promoting undercutting and calving, and hence, possibly increase glacier flow rates (Pimentel et al. 2017, Straneo, 2017). Subaqueous melting has increased in the past decades in Greenland and it is believed to be a result of warmer subsurface ocean waters in the Arctic, however its effect on individual glaciers depends on additional factors as well (Moon et al., 2018).

Ice mélange and its influence on glacier flow has also been in scientific interest recently. It was found that the back-stress exerted by the ice mélange is an important factor in regulating seasonal terminus advance and retreat, mainly by filling the fjord and thereby blocking the free passage of icebergs, preventing calving (Otero et al., 2017).

*Larsen et al., 2016* argues that since UPE1 grounded in 2010, flow accelerations after this year are probably unrelated to ocean temperature fluctuations. Moreover, if the thinning rates remain high, further retreat of the glacier front from the ocean interface is likely.

## Conclusion and future work

---

This thesis covers topics that are increasingly more of both scientific and of public interest, such as glacier flow acceleration, intensifying ice loss from the Greenland ice sheet, the possible causes for these phenomena and future prospects regarding their effect on global climate and sea level, and ultimately on humanity.

In order to establish possible links between glacier velocity fluctuation and climatic changes, the near-terminus region of the northernmost branch of the Upernavik ice stream was investigated.

The georectification and feature tracking toolbox ImGRAFT was applied on time-lapse photographs of the calving front to map velocity changes in the vicinity of the glacier front during August 2014. Results from feature tracking showed faster flow closer to the front than further inland, that is in agreement with prior findings (e.g. Larsen et al. 2016). The highest velocities were found at ca. 370 m away from the glacier front, with a mean daily velocity at 45.63 m/day, that would translate to 16.65 km/yr. Although, this extrapolation is likely to result in inaccurate estimation of annual velocities, as there is a pronounced seasonality in flow speed (Ahlstrøm et al., 2013) and the fastest flow is characteristic for the summer period.

Examining the relationship between weather parameters and flow speed fluctuation revealed significant positive correlations between air temperature and ablation, and between ablation change and flow velocity change. These results were partly supported by previous studies, as the warm induced surface melt increase was shown to promote crevasse fracturing and bed lubrication, and thereby accelerated flow and ablation (Joughin et al., 2008; Otero et al., 2017; Schellenberger et al., 2015).

Calving was reported to cause flow acceleration (Sundal et al., 2013), and vice versa, flow acceleration can stimulate calving rates (Benn et al., 2007). As opposed to these results, other authors reported no coincidence between flow acceleration and glacier front retreat (Lemos et al., 2018) and found a decorrelation between annually averaged velocities and annual mass balance (Van De Wal et al., 2008). It had also been proposed that internal dynamics are the main driver for flow acceleration (Joughin et al., 2008)

It is important to note that the measurements of atmospheric parameters used in this study, and therefore any results based on these data may be biased, as the weather station recording the measurements was not placed on the same branch of the ice stream. This gap may produce skewed results in the analysis, as conditions and the glacier's response to certain factors are often quite dissimilar even in such vicinity.

After evaluating the surface area change at the terminus of UPE 1, an area growth of + 0.0854 km<sup>2</sup> was found between 30.07.2014 – 31.08.2014. representing glacier advance. This advance towards the end of the melt season was expected, in accordance with the findings of *Ahlstrøm et al., 2013*, reporting rapid mid-melt season deceleration at several Greenland glaciers.

The novelty of this thesis lies in the high-resolution aspect of studying flow speed fluctuations both in temporal and in spatial dimensions. This is an advantage because the high frequency, high resolution time-lapse images allow for a close inspection of the calving front that is currently difficult to conduct from space and might reveal changes that may be difficult to notice otherwise; and also a disadvantage as extrapolating any results that were found in this analysis carries a high risk of false conclusions due

to the short time-period in focus and to the spatial limitations, as velocity changes were analyzed only at a short section of the glacier. Drawing conclusions from after comparing the results to other papers also proved to be challenging, as the published studies are generally spanning over a larger time-scale, that potentially has a notable impact on the overall results and conclusions.

A possible future improvement of the results presented in this study could be the extension of the investigated period (poor light-conditions closer to and during winter can pose a limit to the expansion of the data in time).

Another possibility to refine the results of comparable future studies is to synchronize the locations of the analyzed glacier, the camera and the weather station more. Ideally, the camera should be installed at a higher elevation to have a better view-angle with respect to the calving front. If this is not feasible due to the geography of the location, unmanned aerial vehicles such as presented by *Ryan et al., 2014* could be deployed. Regarding the position of the weather station, when possible, best practice would be to place them onto the examined glacier as close to the calving front as possible, so that the measured data would reflect the conditions of the glacier in question best. Installing devices close to the glacier to measure water level and tidal movement could provide additional valuable data.

Given that the Upernavik ice stream has been thoroughly studied in the past years, collecting additional data (or analyzing what is already available but has not yet been processed) could provide a unique and complex insight in terms of glacier behavior which may serve as base for future studies of other glaciers.

Regarding the global relevance of the conducted analysis, the Greenland ice sheet is estimated to have a sea level rise potential of  $7.42 \pm 0.05$  m (Morlighem, 2017). Rates of surface melting in Greenland

were modelled to double in the 21<sup>st</sup> century (Sundal et al., 2011) and the rates of surface mass balance loss are supposedly linked mostly to changes in ablation processes (Mernild et al., 2010). The key drivers of the increased melt water runoff are however not fully understood yet (Van Tricht et al., 2016) and the same is true for calving that is likely controlled by both atmospheric and oceanic processes, however, its main driving mechanisms are yet to be identified and quantified (Otero et al., 2017).

In light of the above and with respect to the immense amounts of ice the Greenland ice sheet contains, considering the consequences of the increased melting and accelerated glacier flow, it is crucial to further study the processes acting at the ice-ocean interface. Gaining more understanding concerning the Greenland ice sheet's response to the current climatic changes is essential, so that appropriate measures can be taken to minimize the negative impacts of the already occurring and predicted changes driven by global warming and importantly, to act on them.

## References

---

1. Ahlstrøm, A. P., Andersen, S. B., Andersen, M. L., Machguth, H., Nick, F. M., Joughin, I., ... Hubbard, A. (2013). Seasonal velocities of eight major marine-terminating outlet glaciers of the Greenland ice sheet from continuous in situ GPS instruments. *Earth System Science Data*, 5(2), 277–287. <https://doi.org/10.5194/essd-5-277-2013>
2. Allison, I., Alley, R. B., Fricker, H. A., Thomas, R. H., & Warner, R. C. (2009). Ice sheet mass balance and sea level. *Antarctic Science*, 21(5), 413–426. <https://doi.org/10.1017/S0954102009990137>
3. Andresen, C. S., Kjeldsen, K. K., Harden, B., Nørgaard-Pedersen, N., & Kjær, K. H. (2014). Outlet glacier dynamics and bathymetry at Upernavik Isstrøm and Upernavik Isfjord, North-West Greenland. *Geological Survey of Denmark and Greenland Bulletin*, (31), 79–82.
4. Benn, D. I., Evans, J. A. (2006). *Glaciers and glaciation*. Oxford University Press
5. Benn, D. I., Warren, C. R., & Mottram, R. H. (2007). Calving processes and the dynamics of calving glaciers. *Earth-Science Reviews*, 82(3–4), 143–179. <https://doi.org/10.1016/j.earscirev.2007.02.002>
6. Bevan, S. L., Luckman, A. J., & Murray, T. (2012). Glacier dynamics over the last quarter of a century at Helheim, Kangerdlugssuaq and 14 other major Greenland outlet glaciers. *Cryosphere*, 6(5), 923–937. <https://doi.org/10.5194/tc-6-923-2012>
7. Box, J. E., & Decker, D. T. (2011). Greenland marine-terminating glacier area changes: 2000–2010. *Annals of Glaciology*, 52(59), 91–98. <https://doi.org/10.3189/172756411799096312>
8. Chylek, P., Dubey, M. K., Lesins, G. (2006). Greenland warming of 1920–1930 and 1995–2005. *Geophysical Research Letters*, (June), 33(11). <https://doi.org/10.1029/2006GL026510>
9. Cook, S., Zwinger, T., Rutt, I. C., Neel, S. O., & Murray, T. (2012). Testing the effect of water in crevasses on a physically based calving model, 53(60), 90–96. <https://doi.org/10.3189/2012AoG60A107>
10. Cuffey, K. M., Paterson, W. S. B. (2010) *The physics of glaciers*, 4<sup>th</sup> edition. Elsevier
11. Dam, G., Søndersholm, M., Larsen, L. M., Pedersen, G. K., Midtgaard, H. H., Nøhr-Hansen, H., Pedersen, A. K. (2009). Lithostratigraphy of the Cretaceous–Paleocene Nuussuaq Group, Nuussuaq Basin, West Greenland. *Geological Survey of Denmark and Greenland Bulletin*, (19)

12. Haubner, K., Box, J. E., Schlegel, N. J., Larour, E. Y., Morlighem, M., Solgaard, M., ... Larsen, S. H. (2018). Simulating ice thickness and velocity evolution of Upernavik Isstrøm 1849–2012 by forcing prescribed terminus positions in ISSM. *The Cryosphere Discussions*, (July), 1–16. <https://doi.org/https://doi.org/10.5194/tc-2017-121>
13. Hofer, S., Bamber, J., Tedstone, A., & Fettweis, X. (2017). Decreasing clouds drive mass loss on the Greenland Ice Sheet. *EGU General Assembly Conference Abstracts*, 19, 5086.
14. Howat, I. M. (2007). Rapid Changes in Ice Discharge from. *Science*, 1559(2007), 5–8. <https://doi.org/10.1126/science.1138478>
15. Howat, I. M., & Eddy, A. (2011). Multi-decadal retreat of Greenland ' s marine-terminating glaciers. *Journal of Glaciology*, 57(203), 389–396. <https://doi.org/10.3189/002214311796905631>
16. IPCC. (2013). Summary for Policymakers. *Climate Change 2013: The Physical Science Basis. Contribution of Working Group I to the Fifth Assessment Report of the Intergovernmental Panel on Climate Change*, 33. <https://doi.org/10.1017/CBO9781107415324>
17. JF, Nye (1952). The mechanics of glacier flow. *Journal of Glaciology*, 2(12), 82–93. <https://doi.org/10.3198/1952JoG2-12-82-93>
18. Joughin, I., Das, S. B., King, M. A., Smith, B. E., Howat, I. M., & Moon, T. (2008). Seasonal Speedup Along Flank of the Greenland Ice Sheet the Western. *Science (New York, N.Y.)*, 320(5877), 781–783.
19. Joughin, I., Smith, B. E., Howat, I. M., Scambos, T., & Moon, T. (2010). Greenland flow variability from ice-sheet-wide velocity mapping, 56(197), 415–430.
20. Khan, S. A., Kjær, K. H., Korsgaard, N. J., Wahr, J., Joughin, I. R., Timm, L. H., ... Babonis, G. (2013). Recurring dynamically induced thinning during 1985 to 2010 on Upernavik Isstrøm, West Greenland. *Journal of Geophysical Research: Earth Surface*, 118(1), 111–121. <https://doi.org/10.1029/2012JF002481>
21. Knight, P.G. (1999). *Glaciers*. Stanley Thornes Ltd.
22. Knight, P.G. (2006), *Glacier science and environmental change*. Blackwell Science Ltd.
23. Larsen, S. H., Khan, S. A., Ahlstrøm, A. P., Hvidberg, C. S., Willis, M. J., & Andersen, S. B. (2016). Increased mass loss and asynchronous behavior of marine-terminating outlet glaciers at Upernavik Isstrøm, NW Greenland.

- Journal of Geophysical Research: Earth Surface*, 121(2), 241–256. <https://doi.org/10.1002/2015JF003507>
24. Lemos, A., Shepherd, A., Mcmillan, M., Hogg, A. E., Hatton, E., & Joughin, I. (2018). Ice velocity of Jakobshavn Isbræ, Petermann Glacier, Nioghalvfjerdingsfjorden and Zachariæ Isstrøm, 2015-2017, from Sentinel 1-a/b SAR imagery. *The Cryosphere Discussions*, (February).
  25. Mankoff, K. D., Straneo, F., Cenedese, C., Das, S. B., Richards, C. G., Singh, & Hanumant. (2016). Structure and dynamics of a subglacial discharge plume in a Greenlandic fjord. *Journal of Geophysical Research: Oceans*, 121(12), 8670–8688. <https://doi.org/10.1002/2016JC011764>.Received
  26. McMillan, M., Leeson, A., Shepherd, A., Briggs, K., Armitage, T. W. K., Hogg, A., ... Gilbert, L. (2016). A high-resolution record of Greenland mass balance. *Geophysical Research Letters*, 43, 7002–7010. <https://doi.org/10.1002/2016GL069666>.Received
  27. Mernild, S. H., Liston, G. E., Hiemstra, C. A., & Christensen, J. H. (2010). Greenland Ice Sheet Surface Mass-Balance Modeling in a 131-Yr Perspective, 1950–2080. *Journal of Hydrometeorology*, 11(1), 3–25. <https://doi.org/10.1175/2009JHM1140.1>
  28. Messerli, A., & Grinsted, A. (2015). Image georectification and feature tracking toolbox: ImGRAFT. *Geoscientific Instrumentation, Methods and Data Systems*, 4(1), 23–34. <https://doi.org/10.5194/gi-4-23-2015>
  29. Moon, T., & Joughin, I. (2008). Changes in ice front position on Greenland's outlet glaciers from 1992 to 2007. *Journal of Geophysical Research: Earth Surface*, 113(2), 1–10. <https://doi.org/10.1029/2007JF000927>
  30. Moon, T., Joughin, I., Smith, B., & Howat, I. (2012). 21st-century evolution of Greenland outlet glacier velocities. *Science*, 336(6081), 576–578. <https://doi.org/10.1126/science.1219985>
  31. Moon, T., Joughin, I., Smith, B., van den Broeke, M. R., van de Berg, W., Noel, B., & Usher, M. (2014). Distinct patterns of seasonal Greenland velocity. *Geophysical Research Letters*, 41, 7209–7216. <https://doi.org/doi:10.1002/2014GL061836>.
  32. Moon, T., Joughin, I., & Smith, B. (2015). Earth Surface. *Journal of Geophysical Research: Earth Surface*, 120(5), 1–16. <https://doi.org/10.1002/2015JF003494>.Received
  33. Moon, T. (2017). Saying goodbye to glaciers, <http://science.sciencemag.org/content/356/6338/580>

34. Moon, T., Ahlstrøm, A., Goelzer, H., Lipscomb, W., & Nowicki, S. (2018). Rising Oceans Guaranteed : Arctic Land Ice Loss and Sea Level Rise, *Current Climate Change Reports*, (4), 211–222. <https://doi.org/10.1007/s40641-018-0107-0>
35. Morlighem, M. (2017). Special Section : BedMachine v3 : Complete Bed Topography and Ocean Bathymetry Mapping of Greenland From Multibeam. *Geophysical Research Letters*, 44, 1–11. <https://doi.org/10.1002/2017GL074954>
36. Morlighem, M., Rignot, E., Mouginot, J., Seroussi, H., & Larour, E. (2014). Deeply incised submarine glacial valleys beneath the Greenland ice sheet. *Nature Geoscience*, 7(6), 418–422. <https://doi.org/10.1038/ngeo2167>
37. Morlighem, M., Williams, C. N., Rignot, E., An, L., Arndt, J. E., Bamber, J. L., ... Zinglensen, K. B. (2017). BedMachine v3: Complete Bed Topography and Ocean Bathymetry Mapping of Greenland From Multibeam Echo Sounding Combined With Mass Conservation. *Geophysical Research Letters*, 44(21), 11,051–11,061. <https://doi.org/10.1002/2017GL074954>
38. Müller, B. F., & Iken, A. (1963). Velocity fluctuations and water regime of Arctic valley glaciers by Fritz Müller and Almut Iken (Axel Heiberg Expedition, McGill University, Montreal, Canada). *Arctic*, 68–75.
39. Murray, T., Scharrer, K., James, T. D., Dye, S. R., Hanna, E., Booth, A. D., ... Huybrechts, P. (2010). Ocean regulation hypothesis for glacier dynamics in southeast Greenland and implications for ice sheet mass changes. *Journal of Geophysical Research: Earth Surface*, 115(3), 1–15. <https://doi.org/10.1029/2009JF001522>
40. Nick, F. M., Luckman, A., Vieli, A., Van Der Veen, C. J., Van As, D., Van De Wal, R. S. W., ... Floricioiu, D. (2012). The response of Petermann Glacier, Greenland, to large calving events, and its future stability in the context of atmospheric and oceanic warming. *Journal of Glaciology*, 58(208), 229–239. <https://doi.org/10.3189/2012JoG11J242>
41. Otero, J., Navarro, F. J., Lapazaran, J. J., Welty, E., Puczko, D., & Finkelnburg, R. (2017). Modeling the controls on the front position of a tidewater glacier in Svalbard, 5(April), 1–11. <https://doi.org/10.3389/feart.2017.00029>
42. Overland, J.E., Hanna, E., Hanssen-Bauer, I., Kim, S.J., Walsh, J., Wang, M., Bhatt, U.S., Thoman, R.L. (2016). Surface air temperature [in Arctic Report Card 2016], <http://www.arctic.noaa.gov/Report-Card>
43. Paterson, W. S. B. (2002) *The physics of glaciers*, 3<sup>rd</sup> edition. Butterworth-Heinemann

44. Pimentel, S., Flowers, G. E., Sharp, M. J., Danielson, B., Copland, L., Van Wychen, W., ... Kavanaugh, J. L. (2017). Modelling intra-annual dynamics of a major marine-terminating Arctic glacier. *Annals of Glaciology*, 58(74), 118–130. <https://doi.org/10.1017/aog.2017.23>
45. Rignot, E., Fenty, I., Xu, Y., Cai, C., Velicogna, I., Cofaigh, C., ... Duncan, D. (2016). Bathymetry data reveal glaciers vulnerable to ice-ocean interaction in Uummannaq and Vaigat glacial fjords, west Greenland. *Geophysical Research Letters*, 43(6), 2667–2674. <https://doi.org/10.1002/2016GL067832>
46. Rignot, E., & Mouginot, J. (2012). Ice flow in Greenland for the International Polar Year 2008-2009. *Geophysical Research Letters*, 39(11), 1–7. <https://doi.org/10.1029/2012GL051634>
47. Rignot, E., Velicogna, I., Van Den Broeke, M. R., Monaghan, A., & Lenaerts, J. (2011). Acceleration of the contribution of the Greenland and Antarctic ice sheets to sea level rise. *Geophysical Research Letters*, 38(5), 1–6. <https://doi.org/10.1029/2011GL046583>
48. Ryan, J., Hubbard, A., & Carr, R. (2014). Repeat UAV photogrammetry to assess calving front dynamics at a large outlet glacier draining the Greenland Ice Sheet, (March). <https://doi.org/10.5194/tcd-8-2243-2014>
49. Scambos, T. A., Bell, R. E., Alley, R. B., Anandakrishnan, S., Bromwich, D. H., Brunt, K., ... Yager, P. L. (2017). How much, how fast?: A science review and outlook for research on the instability of Antarctica's Thwaites Glacier in the 21st century. *Global and Planetary Change*, 153(April), 16–34. <https://doi.org/10.1016/j.gloplacha.2017.04.008>
50. Schaffer, J., Timmermann, R., Erik Arndt, J., Savstrup Kristensen, S., Mayer, C., Morlighem, M., & Steinhage, D. (2016). A global, high-resolution data set of ice sheet topography, cavity geometry, and ocean bathymetry. *Earth System Science Data*, 8(2), 543–557. <https://doi.org/10.5194/essd-8-543-2016>
51. Schellenberger, T., Dunse, T., Käab, A., Kohler, J., & Reijmer, C. H. (2015). Surface speed and frontal ablation of Kronebreen and Kongsbreen , NW Svalbard , from SAR offset tracking, (2003), 2339–2355. <https://doi.org/10.5194/tc-9-2339-2015>
52. Seale, A., Christoffersen, P., Mugford, R. I., & O'Leary, M. (2011). Ocean forcing of the Greenland Ice Sheet: Calving fronts and patterns of retreat identified by automatic satellite monitoring of eastern outlet glaciers.

- Journal of Geophysical Research: Earth Surface*, 116(3), 1–16. <https://doi.org/10.1029/2010JF001847>
53. Shepherd, A., Wingham, D., & Rignot, E. (2004). Warm ocean is eroding West Antarctic Ice Sheet. *Geophysical Research Letters*, 31(23), 1–4. <https://doi.org/10.1029/2004GL021106>
  54. Singh, P., Singh, V.P., (2001). Snow and glacier hydrology: Dordrecht, Netherlands, Kluwer Academic Publishers, 742 p.
  55. Tangborn, W.V., (1980), Two models for estimating climate-glacier relationships in the North Cascades, Washington, USA: *Journal of Glaciology*, v. 25, p. 3–21.
  56. Stocker-waldhuber, M., Fischer, A., Helfricht, K., & Kuhn, M. (2018). Ice flow velocity as a sensitive indicator of glacier state, *The Cryosphere Discussions*, (March), 1–18. <https://doi.org/10.5194/tc-2018-37>
  57. Sugiyama, S., Sakakibara, D., Tsutaki, S., Maruyama, M., & Sawagaki, T. (2015). Glacier dynamics near the calving front of Bowdoin Glacier, northwestern Greenland. *Journal of Glaciology*, 61(226), 223–232. <https://doi.org/10.3189/2015JoG14J127>
  58. Sundal, A. V., Shepherd, A., Nienow, P., Hanna, E., Palmer, S., & Huybrechts, P. (2011). Melt-induced speed-up of Greenland ice sheet offset by efficient subglacial drainage. *Nature*, 469(7331), 521–524. <https://doi.org/10.1038/nature09740>
  59. Sundal, A. V., Shepherd, A., Broeke, M. V. A. N. D. E. N., Angelen, J. V. A. N., Gourmelen, N., & Park, J. (2013). Controls on short-term variations in Greenland glacier dynamics, *Journal of Glaciology*, 59(217), 883–892. <https://doi.org/10.3189/2013JoG13J019>
  60. Tedesco, M., Fettweis, X., Mote, T., Wahr, J., Alexander, P., Box, J. E., Wouters, B. (2013). Evidence and analysis of 2012 Greenland records from spaceborne observations, a regional climate model and reanalysis data. *The Cryosphere*, (April), 615-630. <https://doi.org/10.5194/tc-7-615-2013>
  61. Ten Brink, N. W. (1974). Glacio-Isostasy: New data from West Greenland and geophysical implications. *Bulletin of the Geological Society of America*, 85(2), 219–228. [https://doi.org/10.1130/0016-7606\(1974\)85<219:GNDFWG>2.0.CO;2](https://doi.org/10.1130/0016-7606(1974)85<219:GNDFWG>2.0.CO;2)
  62. Van De Wal, R. S. W., Boot, W., van den Broeke, M. R., Smeets, C. J. P. P., Reijmer, C. H., Donker, J. J. A.,

- Oerlemans, J. (2008). Large and rapid melt-induced velocity changes in the ablation zone of the Greenland Ice sheet. *Science*, 321(July), 111–114.
63. van den Broeke, M. R., Bamber, J., Ettema, J., Rignot, E., Schrama, E., van de Berg, W., ... Wouters, B. (2009). Partitioning recent Greenland mass loss. *Science*, 326(984), 984–986.  
<https://doi.org/DOI: 10.1126/science.1178176>
64. Van Tricht, K., Lhermitte, S., Lenaerts, J. T. M., Gorodetskaya, I. V., L'Ecuyer, T. S., Noël, B., ... Van Lipzig, N. P. M. (2016). Clouds enhance Greenland ice sheet meltwater runoff. *Nature Communications*, 7(May 2015).  
<https://doi.org/10.1038/ncomms10266>
65. Velicogna, I., Sutterley, T. C., & Van Den Broeke, M. R. (2014). Regional acceleration in ice mass loss from Greenland and Antarctica using GRACE time-variable gravity data. *Geophysical Research Letters*, 41(22), 8130–8137. <https://doi.org/10.1002/2014GL061052>
66. Walter, J. I., Box, J. E., Tulaczyk, S., Brodsky, E. E., Howat, I. M., Ahn, Y., & Brown, A. (2012). Oceanic mechanical forcing of a marine-terminating greenland glacier. *Annals of Glaciology*, 53(60), 181–192.  
<https://doi.org/10.3189/2012AoG60A083>
67. Wang, K., & Dickinson, R. E. (2013). Global atmospheric downward longwave radiation at the surface from ground-based observations, satellite retrievals, and reanalyses, (2012), 150–185.  
<https://doi.org/10.1002/rog.20009.1.INTRODUCTION>
68. Willis, I. C., & Place, D. (n.d.). Intra-annual variations in motion : a review, 61–106.

# Appendix

---

## Camera data

Position:

- Lat: 73.00088889
- Lon: -54.29102778

Model: NIKON D3200 S/N: 3227304

Image size: 4512 × 3000

Resolution: 300 Pixels pr. Inch

Lens: 24.0 mm f/2.8

Focal Length: 24.0 mm

---

## MATLAB codes

### Camera fitting:

```
close all
%load data

A=imread('d:\GEO\Msc\images\UPE cam 2015 all\Upernavik_aug2014_628.JPG');
gcpA=xlsread('D:\GEO\Msc\GCP_dora_.xlsx');
gcpA=gcpA(:,[1 3 2 4 5 6]);

limx=[-304251 -295785];
limy=[-1823491 -1830478];
file='D:/GEO/Msc/cosmo ice mask/merged_filled.tif';
[Z,x,y,I]=geoimread(file,limx,limy); % [A,x,y,I] = geoimread(...) also returns pixel center
coordinates (x,y) of the output image and a geotiff info structure I.

[X,Y]=meshgrid(x,y); % [X,Y] = meshgrid(x,y) returns 2-D grid coordinates based on the
coordinates contained in vectors x and y

ix=isnan(gcpA(:,4)); % TF = isnan(A) returns an array the same size as A containing logical
1 (true) where the elements of A are NaNs- not a number- and logical 0 (false) where they
are not
```

```

gcpA(ix,4)=interp2(X,Y,Z,gcpA(ix,2),gcpA(ix,3));

dem=GRIDObj(X,Y,Z); % -from TopoToolbox
dem=inpaintnans(dem);
Z=dem.Z;

%camera location as given in practice:
camxyz=[-299429.30 -1830325.19];
d=sqrt((X-camxyz(1)).^2+(Y-camxyz(2)).^2);
nearix=find(d<60);
[camxyz(3),ix]=max(Z(nearix));
camxyz(1)=X(nearix(ix));
camxyz(2)=Y(nearix(ix));
camxyz(3)=camxyz(3)+10;
% camxyz(3)=interp2(X,Y,Z,camxyz(1),camxyz(2),'spline')+17.5;

%initial guess camera parameters: (also from practice)

FocalLength=24; %mm
SensorSize=[23.6 15.8]; %mm: Nikon D200 for EIS on Upernavik
imgsz=size(A); %size of image in pixels [#rows, #columns]
f=imgsz([2 1]).*(FocalLength./SensorSize); %focal length in pixel units (two
%element vector [fx,fy])

camA=camera(camxyz,size(A),[120 0 0]*pi/180,f); %approximate look direction.

rmse=0;aic=0; % root-mean-square error, aic= Akaike's Information Criterion for estimated
model
camA.xyz(3)
[camA,rmse,aic]=camA.optimizecam(gcpA(:,2:4),gcpA(:,5:6),'0010011111001000000');
fprintf('reprojectionerror=%3.1fpx AIC:%4.0f\n',rmse,aic)
camA.xyz(3)

save('U-fittedcamera','camA')

image(A)
axis equal off tight
hold on

%project the DEM onto the camera plane
[uvDEM,~,inframe]=camA.project([X(:),Y(:),Z(:)]);

%Hide DEM points that are not visible from the camera:
vis=voxelviewshed(X,Y,Z,camA.xyz);
uvDEM(~(inframe&vis(:)),:)=nan;

%show DEM as a mesh with labelled contours on top.
mesh(reshape(uvDEM(:,1),size(Z)),reshape(uvDEM(:,2),size(Z)),Z*0,'facecolor','none','edgecolor', [.7 .7 1]*.7)
[c,h]=contour(reshape(uvDEM(:,1),size(Z)),reshape(uvDEM(:,2),size(Z)),Z,[2600:50:3000],'k');
clabel(c,h)

%Show GCPs and reprojected GCPs
uvGCP=camA.project(gcpA(:,2:4));
h=plot(uvGCP(:,1),uvGCP(:,2),'ro',gcpA(:,5),gcpA(:,6),'m*','markerfacecolor','w');
legend(h([2 1]),'UV of GCP','projection of GCPs','location','northeast')
title(sprintf('Projection of ground control points. RMSE=%3.1fpx',rmse))

```

```

figure

visible=voxelviewshed(X,Y,Z,camA.xyz);

A=im2double(A);
[uv,~,inframe]=camA.project([X(:) Y(:) Z(:)]);
uv(~inframe|~visible(:),:)=nan;

rgb=nan(size(Z,1),size(Z,2),1);
for jj=1:3
    rgb(:, :, jj)=reshape(interp2(A(:, :, jj),uv(:, 1),uv(:, 2)),size(X));
end
showimg(x,y,rgb);

```

---

## Tracking pixel displacement

```

function trackpair(idA,idB)

if nargin==0
    idA=628;
    idB=649;
end

folder='D:/GEO/Msc/images/UPE cam 2015 all/';
fA=dir(fullfile(folder,sprintf('*_%03.0f.jpg',idA))); %Build full file name from parts
fB=dir(fullfile(folder,sprintf('*_%03.0f.jpg',idB)));
dt=fB.datenum-fA.datenum; % Convert date and time to serial date number

A = imread(fullfile(fA.folder,fA.name));
B = imread(fullfile(fB.folder,fB.name));

[pu,pv] = meshgrid(1100:25:4500,1300:25:2500);

chipsz=61;
maxdisplacement=dt*100;

[du,dv,C,Cnoise] =
templatematch(A,B,pu,pv,'templatewidth',chipsz,'searchwidth',round(chipsz+maxdisplacement*2)
,'method','oc');

f=figure(25);clf
V=sqrt(du.^2+dv.^2)/dt;
imagesc(V/dt);
caxis([0 60])
title(sprintf('%03.0f %03.0f dt=%.1fh',idA,idB,dt*24))

outputfolder='D:\GEO\Msc\pixel displacement2';
datafile=fullfile(outputfolder,sprintf('%03.0f_%03.0f.mat',idA,idB));
imagefile=strrep(datafile,'.mat','.png');

save(datafile,'du','dv','C','Cnoise','fA','fB','dt','pu','pv','idA','idB')

saveas(f,imagefile)

```

---

## Looping the images one after the other

```
imagelist=load('D:\GEO\Msc\image_list2.txt'); % 1 image/day at 14:40

for ix=1:length(imagelist)-1
    trackpair(imagelist(ix),imagelist(ix+1))
end
```

---

## Pairing velocities between two consecutive days:

```
function [Vx,Vy,xyzA,keep]=pairvelocity(fpair)

if nargin==0
    fpair='D:\GEO\Msc\pixel displacement2\190_214.mat';
end

load(fpair)

load('U-fittedcamera');

persistent dem
if isempty(dem)
    limx=[-304251 -295785];
    limy=[-1823491 -1830478];
    file='D:\GEO\Msc\cosmo ice mask\merged_filled.tif';
    [dem.Z,dem.x,dem.y,dem.I]=geoimread(file,limx,limy);
    dem.Z=double(dem.Z);
    fcirc=fspecial('disk',2); %Create predefined 2-D filter
    dem.Z=log(imfilter(exp(dem.Z),fcirc)); %B = imfilter(A,h) filters the multidimensional
array A with the multidimensional filter h.
    [dem.X,dem.Y]=meshgrid(dem.x,dem.y);
end

uvA=[pu(:) pv(:)];
uvB=[pu(:)+du(:) pv(:)+dv(:)];

xyzA=camA.invproject(uvA,dem.X,dem.Y,dem.Z);
xyzB=camA.invproject(uvB,dem.X,dem.Y,dem.Z);
V=(xyzB-xyzA)/dt;

Vx=reshape(V(:,1),size(pu));
Vy=reshape(V(:,2),size(pu));

inconsistent=sqrt((medfilt2(Vx)-Vx).^2+(medfilt2(Vy)-Vy).^2); %2-D median filtering
```

```

maxV=200;%m/d
keep=find((inconsistent<3)&(sqrt(Vx.^2+Vy.^2)<maxV));%within 3 m/day

if nargout==0
    figure(71)
    [S,sx,sy,Is]=geoimread('D:\GEO\Msc\Sentinel\Sentinel-2 L1C 3413 from 2016-06-
06_TIFF.tiff');
    showing(sx,sy,im2single(S))
    hold on
    plot(xyzA(:,1),xyzA(:,2),'b.')
    quiver(xyzA(keep,1),xyzA(keep,2),V(keep,1),V(keep,2),6,'r') %A quiver plot displays
velocity vectors as arrows with components (u,v) at the points (x,y).
    axis equal

    clear Vx Vy keep xyzA
end

```

---

## Calendar plot:

```

line=[ -299349 -1828392; -300445 -1829089];

N=100;
linex=linspace(line(1,1),line(2,1),N)';
liney=linspace(line(1,2),line(2,2),N)';
distance=sqrt((linex(1)-linex).^2+(liney(1)-liney).^2);
uv=diff(line);
uv=uv./sqrt(uv(1).^2+uv(2).^2);

d=dir('D:\GEO\Msc\pixel displacement2\*.mat');

V=nan(length(distance),length(d));
idA=nan(1,length(d));
idB=nan(1,length(d));
dt=nan(1,length(d));

for ii=1:length(d)
    fpair = fullfile('D:\GEO\Msc\pixel displacement2\',d(ii).name);
    p=load(fpair,'dt','idA','idB');
    [Vx,Vy,xyzA,keep]=pairvelocity(fpair);
    idA(ii)=p.idA;
    idB(ii)=p.idB;
    dt(ii)=p.dt;

    Vim=(Vx*uv(1)+Vy*uv(2)); %project to get V along line direction
    Vim(~keep)=nan;
    F=scatteredInterpolant(xyzA(:,1),xyzA(:,2),Vim(:));
    V(:,ii)=F(linex,liney);

end
figure(95)
imagesc(idA,distance,(V))
xticks([001 022 046 070 094 118 142 165 190 214 238 263 285 311 331 352 374 393 415 445 455
473 494 515 534 553 571 590 609 628 ])

```

```

xticklabels({'02','03','04','05','06','07','08','09','10','11','12','13','14','15','16','17',
,'18','19','20','21','22','23','24','25','26','27','28','29','30','31'});
xtickangle(90);
c=colormap;
c(1,:)=1;
colormap(c);
colorbar
caxis([0 100])

```

---

## Comparison to Terra SAR-X:

```

line=[ -299349 -1828392; -300445 -1829089];

d=dir('D:\GEO\Msc\pixel displacement2\*.mat');

fpair = 'D:\GEO\Msc\pixel displacement2\190_214.mat';
p=load(fpair,'dt','idA','idB');
[Vx,Vy,xyzA,keep]=pairvelocity(fpair);
V=sqrt(Vx.^2+Vy.^2);

[tvx,xt,yt,It]=geotiffread('D:\GEO\Msc\Measures\TSX_W72.90N_22Aug14_02Sep14_20-34-03_vx_v1.2.tif');tvx(tvx<-1e9)=nan;
[tv,yt,xt,It]=geotiffread('D:\GEO\Msc\Measures\TSX_W72.90N_22Aug14_02Sep14_20-34-03_vy_v1.2.tif');tv(tv<-1e9)=nan;
[XT,YT]=meshgrid(xt,yt);

tv=sqrt(tvx.^2+tv.^2)/365.25;

subplot(1,2,1)
alphawarp(XT,YT,tv,~isnan(tv))
colormap(jet)
axis xy equal
caxis([0 40]);
hold on
plot(line(:,1),line(:,2),'k','linewidth',3);
xlim([-304767 -294267])
ylim([-1840505 -1821327])
V(~keep(:))=nan;
V(V(:)>30)=nan;

subplot(1,2,2)
hold on
isT=repmat(isnan(tv),1,1,3);
imagesc(xt,yt,.9+isT*.1);hold on
scatter(xyzA(:,1),xyzA(:,2),80,V(:),'.')
hold on
axis xy equal
caxis([0 40]);

plot(line(:,1),line(:,2),'k','linewidth',3);
xlim([-304767 -294267])
ylim([-1840505 -1821327])
set(gca,'yticklabel',[])
linkaxes(findobj(gcf,'type','axes'),'xy')

```

```
pos=get(gca,'position');
axes('position',[pos(1)+.05 pos(2)+0.1 pos(3)-.1 .05])
V=linspace(0,40,200);
imagesc(V,0,V)
caxis([0 40])
set(gca,'ytick',[])

return
```

---

## Correlating parameters (substitute for the desired parameter):

```
q=load('airT_cloud.txt');
q(isnan(q(:,1)),:)=[];

fmoving = @(x)imfilter(x,[1;1;1]/3,'replicate');
fhi = @(x)x-fmoving(x);

figure(1)

x=q(:,2);
y=q(:,1);
scatter(x,y,'k','filled')
[C,P]=corr(x,y)
text(.9,.9,sprintf('C=%0.2f
_{P=%0.3f}'),C,P),'units','normalized','horizontalalignment','right')
xlabel('Cloud cover')
ylabel('Air T (°C)')
```

---

# Weather station data

